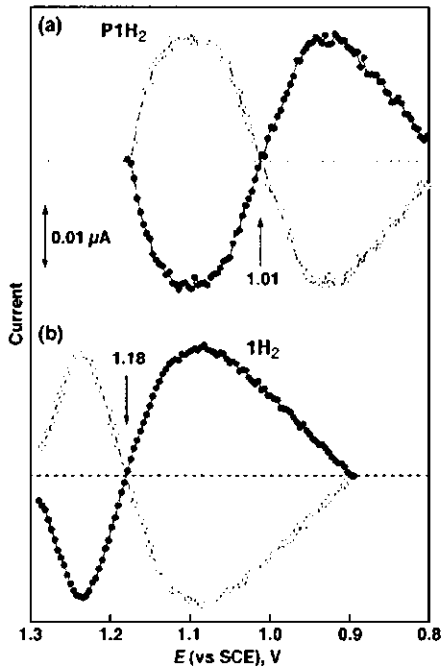

Figure 4. SHACVs of (a) $\mathbf{P1H_2}$ and (b) $\mathbf{1H_2}$ in deaerated MeCN containing 0.1 M TBAP at 298 K. Scan rate, 4 mV s^{-1}; working electrode, Pt.

SHACV method was applied to determine the one-electron oxidation potentials (E_{ox}^0) of $\mathbf{P1H_2}$ and $\mathbf{1H_2}$ in deaerated MeCN containing 0.1 M TBAP at 298 K. Figure 4 shows the SHACV of $\mathbf{P1H_2}$ and $\mathbf{1H_2}$. The E_{ox}^0 value of $\mathbf{P1H_2}$ thus determined (1.01 V vs SCE) is significantly more negative than that of $\mathbf{1H_2}$ (1.18 V vs SCE) as expected above. Thus, $\mathbf{P1H_2}$ may undergo one-electron oxidation by cumylperoxyl radical more easily than $\mathbf{1H_2}$, showing excellent radical scavenging abilities.

Discussion

The primary goal of this project is to develop a novel antioxidant, which can be positively utilized for clinical treatment and/or chemoprevention of diseases associated with ROS. There are two kinds of strategy in considering the development of synthetic antioxidants: one is a design of a new type of antioxidant, the structure of which is different from the natural antioxidant, and the other is a modification of natural antioxidants to improve its antioxidative capacities. A recent topic on the synthetic antioxidants is a development and clinical application of edaravone (3-methyl-1-phenyl-2-pyrazolin-5-one, MCI-186). Edaravone has been reported to show potent free radical scavenging actions toward ROS, such as $O_2^{\bullet-}$, H_2O_2, and HClO, which may be involved in the tissue destructive effects of reperfusion after ischemia (*54*−*56*). As a neuroprotective agent, edaravone has been clinically prescribed in Japan since 2001 to treat patients with cerebral ischemia. Regarding flavonoids, there are many reports for the synthetic derivatives to exert prominent chemopreventive effects toward oxidative stress derived injury. However, only a few studies on the synthetic flavonoids, which were aimed at the improved radical scavenging ability, have been reported. Flavopiridol is a chlorinated derivative of flavone, which is currently in clinical development for the treatment of advanced cancer, including ovarian cancer (*57*, *58*). Flavopiridol is an inhibitor of cycline dependent kinases to modulate cell cycle (*59*), and radical scavenging mechanism is not involved in the expression of anticancer effects of this compound.

The planar catechin ($\mathbf{P1H_2}$), which has been detected in mere trace amounts in nature (*60*), is easily synthesized by the reaction of $\mathbf{1H_2}$ and acetone (*26*). The ability of $\mathbf{P1H_2}$ to scavenge oxygen centered radical, such as galvinoxyl radical, is excellent as compared to that of (+)-catechin and its complete inhibition of oxidative DNA damage induced by metal catalyzed generation of hydroxyl radical (*26*), as well. Therefore, $\mathbf{P1H_2}$ may exert its antioxidative capacities by scavenging reactive oxygen radicals in many types of biologically generating systems. The present study was focused on the reaction of $\mathbf{P1H_2}$ to cumylperoxyl radical, a model radical of lipid peroxyl radical formed in a radical chain reaction of lipid peroxidation. The processes of lipid peroxidation concomitant with the formation of lipid peroxyl radicals are detrimental to the viability of the cell. The biophysical consequences of peroxidation on membrane phospholipids can be both extensive and highly destructive, provoking diseased states such as atherosclerosis, heart attacks, cancer, ischaemia/repulsion injury, and even the aging process as a whole (*61*). The ability of antioxidant to scavenge peroxyl radicals and block lipid peroxidation raises the possibility that it may protect against the many types of free radical associated diseases. As compared with $\mathbf{1H_2}$, $\mathbf{P1H_2}$ showed strong radical scavenging ability toward cumylperoxyl radical formed via a radical chain process, as well as the predominant radical scavenging reaction of $\mathbf{P1H_2}$ to galvinoxyl radical. Lipid peroxyl radical formed by the reaction between a lipid radical and a molecular oxygen is essential for autoxidation of lipid. The peroxyl radical abstracts an allylic hydrogen atom from an adjacent polyunsaturated fatty acid, resulting in a lipid hydroperoxide and a second lipid radical. Therefore, $\mathbf{P1H_2}$ may act as an effective terminator by means of scavenging free radicals in autoxidation of lipids.

Considering the antioxidative mechanism to scavenge peroxyl radical, there are two possibilities in the mechanism of hydrogen transfer reactions, i.e., a one step hydrogen atom transfer or electron transfer followed by proton transfer. The hydrogen transfer reaction from $\mathbf{P1H_2}$ to cumylperoxyl radical accelerated in the presence of the metal ion, indicating that the hydrogen transfer reaction proceeded by the two step reaction, that is, electron transfer from $\mathbf{P1H_2}$ to cumylperoxyl radical followed by proton transfer from $\mathbf{P1H_2}^{\bullet+}$. Vitamin E is a typical antioxidant to terminate lipid peroxidation, and the hydrogen transfer reaction proceeds via a one step hydrogen atom transfer process, which is due to no effect of metal ion on the hydrogen transfer rate from vitamin E analogue to galvinoxyl radical (*62*). On the other hand, in the case of $\mathbf{1H_2}$, the hydrogen transfer reaction proceeds via electron transfer from $\mathbf{1H_2}$ to oxyl radical followed by proton transfer rather than via a one step hydrogen atom transfer (*31*), as the case of present results of the $\mathbf{P1H_2}$. The one electron oxidation potential investigated by the SHACV indicated that the electrochemical oxidation of $\mathbf{P1H_2}$ was easier to progress in comparison with $\mathbf{1H_2}$. The electron transfer mechanism for the radical scavenging reaction of $\mathbf{P1H_2}$ is probably a consequence of its electrochemical ease for one electron oxidation. Judging from the one electron oxidation po

tential of $\mathbf{P1H_2}$ that is higher than the one electron reduction potential of cumylperoxyl radical ($E^{\circ}_{red} = 0.65$ V vs SCE) (*63*), the free energy changes of electron transfer from $\mathbf{P1H_2}$ to cumylperoxyl radical are positive [ΔG_{et}° (in eV) $= e(E^{\circ}_{ox} - E^{\circ}_{red}) > 0$, where e is elementary charge]; thereby, the electron transfer step is endergonic. In such a case, the initial electron transfer rate (k_{et}) may be the rate determining step in the overall rate of hydrogen transfer, which consists of electron and proton transfer steps. The maximum k_{et} value is evaluated from the ΔG_{et}° value by eq 1, where it is assumed that the activation free energy ($\Delta G_{et}^{\ddagger}$) is equal to ΔG_{et}° (no additional barrier is involved). Z is the frequency factor taken as 1×10^{11} M^{-1} s^{-1}, and k_B is the Boltzmann constant (*64*, *65*).

$$k_{et} = Z \exp(-\Delta G_{et}^{\circ}/k_B T) \qquad (1)$$

The maximum k_{et} value is calculated as 1.2×10^2 M^{-1} s^{-1}, which is the same order of magnitude as the observed k_{III} value (9.0×10^2 M^{-1} s^{-1}). The larger k_{III} value than the k_{et} value indicates that the hydrogen transfer from $\mathbf{P1H_2}$ to cumylperoxyl radical proceeds via a rate determining electron transfer with an interaction between $\mathbf{P1H_2}$ and cumylperoxyl radical. The formation of charge transfer complexes between cumylperoxyl radical and a variety of electron acceptors has been well documented in the literature (*66*, *67*). Thus, the hydrogen transfer may proceed via an inner sphere electron transfer in the charge transfer complex formed between $\mathbf{P1H_2}$ and cumylperoxyl radical. The acceleration of the hydrogen transfer rate in the presence of Sc^{3+} (Figure 3) is ascribed to the promoting effect of Sc^{3+} on the electron transfer step due to the strong binding of Sc^{3+} with cumylperoxyl anion produced in the electron transfer.

In conclusion, the hydrogen transfer from $\mathbf{P1H_2}$ to cumylperoxyl radical generated in radical chain reactions proceeds via an electron transfer reaction and the rate of hydrogen transfer from $\mathbf{P1H_2}$ to cumylperoxyl radical is faster than that from $\mathbf{1H_2}$. The predominance of $\mathbf{P1H_2}$ in the hydrogen transfer reaction is consistent with the electrochemical ease for its one electron oxidation potential. Since $\mathbf{P1H_2}$ is very lipophilic as compared to (+) catechin itself, it is proposed that $\mathbf{P1H_2}$ interacts and penetarates the lipid bilayer giving rise to its maximized antioxidant capacity. Therefore, we believe that $\mathbf{P1H_2}$ may be significantly more effective not only for protecting tissue from the onslaught of the radical species governing peroxidation but also for terminating the autoxidation, which plays in provoking diseased states. Studies are underway to investigate basic biochemical properties of $\mathbf{P1H_2}$ in vivo, as well as to investigate its ability to serve as an antioxidant for the treatment of diseases associated with oxidative stress.

Acknowledgment. This work was partially supported by a Grant in Aid for Scientific Research Priority Area (No. 11228205) and a Grant in Aid for Young Scientist (B) (No. 15790032) from the Ministry of Education, Culture, Sports, Science and Technology, Japan, partly by a Grant (MF 16) from the Organization for Pharmaceutical Safety and Research, and by a Grant in Aid for the Scientific Research (No. 14141201) from the Ministry of Health Labor and Welfare.

References

(1) Marchioli, R. (1999) Antioxidant vitamins and prevention of cardiovascular disease: laboratory, epidemiological and clinical trial data. *Pharmacol. Res. 40*, 227−238.

(2) Colic, M., and Pavelic, K. (2000) Molecular mechanisms of anticancer activity of natural dietetic products. *J. Mol. Med. 78*, 333−336.

(3) Willis, M. S., and Wians, F. H. (2003) The role of nutrition in preventing prostate cancer: a review of the proposed mechanism of action of various dietary substances. *Clin. Chim. Acta 330*, 57−83.

(4) Jadhav, S. J., Nimbalkar, S. S., Kulkarni, A. D., and Madhavi, D. L. (1996) Lipid oxidation in biological and food systems. In *Food Antioxidants* (Madhavi, D. L., Deshpande, S. S., and Salunkhe, D. K., Eds.) pp 5−63, Dekker, New York.

(5) Sies, H. (1987) *Oxidative Stress*, Academic Press, London.

(6) Katzman, R., and Kawas, C. (1994) The epidemiology of dementia and Alzheimer's disease. In *Alzheimer Disease* (Terry, R. D., Katzman, R., and Bick, K. L., Eds.) pp 103−119, Raven Press, New York.

(7) Cody, V., Middleton, E., and Harborne, J. B. (1986) *Plant Flavonoids in Biology and Medicine: Biochemical Pharmacological and Structure−Activity Relationships*, Alan R. Liss, New York.

(8) Middleton, E., Jr., and Kandaswami, C. (1993) The impact of plant flavonoids on mammalian biology: implications for immunity, inflammation and cancer. In *The Flavonoids: Advances in Research Since 1986* (Harborne, J. H., Ed.) pp 619−652, Chapman and Hall, New York.

(9) Rice-Evance, C. A., Miller, N. J., and Paganga, G. (1996) Structure−antioxidant activity relationships of flavonoids and phenolic acids. *Free Radical Biol. Med. 20*, 933−956.

(10) Jovanovic, S. V., Steenken, S., Tosic, M., Marjanovic, B., and Simic, M. G. (1994) Flavonoids as antioxidants. *J. Am. Chem. Soc. 116*, 4846−4851.

(11) Hu, J. P., Calomme, M., Lasure, A., De Bruyne, T., Pieters, L., Vlietinck, A., and Vanden Berghe, D. A. (1995) Structure−activity relationships of flavonoids with superoxide scavenging ability. *Biol. Trace Elem. Res. 47*, 327−331.

(12) Terao, J., Piskula, M., and Yao, Q. (1994) Protective effect of epicatechin, epicatechin gallate and quercetin on lipid peroxidation in phospholipids bilayers. *Arch. Biochem. Biophys. 308*, 278−284.

(13) Morel, J., Lescoat, G., Cogrel, P., Sergent, O., Pasdeloup, N., Brissot, P., Cillard, P., and Cillard, J. (1993) Antioxidant and iron chelating activities of the flavonoids catechin, quercetin and diosmetin on iron loads rat hepatocyte cultures. *Biochem. Pharmacol. 45*, 13−19.

(14) Sugimura, T., Nagao, M., Matsushima, T., Yahagi, T., Seino, Y., Shirai, A., Sawamura, M., Natori, S., Yoshihira, K., Fukuoka, M., and Kuroyanagi, M. (1977) Mutagenicity of flavone dericatives. *Proc. Jpn. Acad. B 53*, 194−197.

(15) Ochiai, M., Nagao, M., Wakabayashi, K., and Sugimura, T. (1984) Superoxide dismutase acts an enhancing factor for quercetin mutagenesis in rat liver cytosol by preventing its decomposition. *Mutat. Res. 129*, 19−24.

(16) Das, A., Wang, J. H., and Lien, E. J. (1994) Carcinogenicity, mutagenicity and cancer preventing activities of flavonoids: a structure system activity relationship (SSAR) analysis. *Prog. Drug Res. 42*, 133−166.

(17) Sahu, S. C., and Washington, M. C. (1991) Effects of antioxidants on quercetin induced nuclear DNA damage and lipid peroxidation. *Cancer Lett. 60*, 259−264.

(18) Duthie, S. J., Johnson, W., and Dobson, V. L. (1997) The effect of dietary flavonoids on DNA damage (strand breaks and oxidized pyrimidines) and growth in human cells. *Mutat. Res. 390*, 141−151.

(19) Verma, A. K., Johnson, J. A., Gould, M. N., and Tanner, M. A. (1988) Inhibition of 7,12-dimethylbenz[*a*]anthracene- and *N*-nitrosomethylurea-induced rat mammary cancer by dietary flavonol quercetin. *Cancer Res. 48*, 5754−5758.

(20) Deschner, E. E., Ruperto, J., Wong, G., and Newmark, H. L. (1991) Quercetin and rutin as inhibitors of azoxymethanol-induced colonic neoplasia. *Carcinogenesis 12*, 1193−1196.

(21) *Toxicology and Carcinogenesis Studies of Quercetin in F344 Rats* (1992) National Toxicology Program (NTP) Technical Report, NTP TR 409, NIH Publication No. 93-147478, National Institutes of Health, Bethesda, MD.

(22) Pamukcu, A. M., Yalciner, S., Hatcher, J. F., and Bryan, G. T. (1980) Quercetin, a rat intestinal and bladder carcinogen present in bracken fern (*Pteridium aquilinum*). *Cancer Res. 40*, 3468−3472.

(23) Kandaswami, C., Perkins, E., Soloniuk, D. S., Drzewiecki, G., and Middleton, E., Jr. (1991) Antiproliferative effects of citrus flavonoids on a human squamous cell carcinoma in vitro. *Cancer Lett. 56*, 147−152.

(24) Yoshikawa, T., Toyokuni, S., Yamamoto, Y., and Naito, Y. (2000) *Free Radical in Chemistry, Biology and Medicine*, OICA International (U.K.) Ltd., London.
(25) Guiso, M., Marra, C., and Cavarischia, C. (2001) Isochromans from 2 (3′,4′ dihydroxy)phenylethanol. *Tetrahedron Lett. 42*, 6531−6534.
(26) Fukuhara, K., Nakanishi, I., Kansui, H., Sugiyama, E., Kimura, M., Shimada, T., Urano, S., Yamaguchi, K., and Miyata, N. (2002) Enhanced radical scavenging activity of a planar catechin analogue. *J. Am. Chem. Soc. 124*, 5952−5953.
(27) Fukuhara, K., Nakanishi, I., Shimada, T., Ohkubo, K., Miyazaki, K., Hakamata, W., Urano, S., Ozawa, T., Okuda, H., Miyata, N., Ikota, N., and Fukuzumi, S. (2003) A planar catechin analogue as a promising antioxidant with reduced prooxidant activity. *Chem. Res. Toxicol. 16*, 81−86.
(28) Russel, G. A. (1973) Reactivity, selectivity, and polar effects in hydrogen atom transfer reactions. In *Free Radicals* (Kochi, J. K., Ed.) pp 275−331, John Wiley & Sons, New York.
(29) Russel, G. A. (1956) The rates of oxidation of aralkyl hydrocarbons. Polar effects in free radical reactions. *J. Am. Chem. Soc. 78*, 1047−1054.
(30) Howard, J. A., Ingold, U. K., and Symonds, M. (1968) Absolute rate constants for hydrocarbon oxidation VIII. Reactions of cumylperoxyl radicals. *Can. J. Chem. 46*, 1017−1022.
(31) Nakanishi, I., Miyazaki, K., Shimada, T., Ohkubo, K., Urano, S., Ikota, N., Ozawa, T., Fukuzumi, S., and Fukuhara, K. (2002) Effects of metal ions distinguishing between one step hydrogen and electron transfer mechanisms for the radical scavenging reaction of (+) catechin. *J. Phys. Chem. A 106*, 11123−11126.
(32) Perrin, D. D., Armarego, W. L. F., and Perrin, D. R. (1988) *Purification of Laboratory Chemicals*, Pergamon Press, Elmsford, New York.
(33) McCord, T. G., and Smith, D. E. (1969) Second harmonic a.c. polarography. Theoretical predictions for systems with first order chemical reactions following the charge transfer step. *Anal. Chem. 41*, 1423−1441.
(34) Bond, A. M., and Smith, D. E. (1974) Direct measurement of $E^0_{1/2}$ with reversible EC electrode processes by second harmonic alternating current polarography and voltammetry. *Anal. Chem. 46*, 1946−1951.
(35) Wasielewski, M. R., and Breslow, R. (1976) Thermodynamic measurements on unsubstituted cyclopropenyl radical and anion, and derivatives by second harmonic alternating current voltammetry of cyclopropenyl cations. *J. Am. Chem. Soc. 98*, 4222−4229.
(36) Arnett, E. M., Amarnath, K., Harvey, N. G., and Cheng, J. P. (1990) Determination and interrelation of bond heterolysis and homolysis energies in solution. *J. Am. Chem. Soc. 112*, 344−355.
(37) Patz, M., Mayr, H., Maruta, J., and Fukuzumi, S. (1995) Reactions of carbocations with π nucleophiles: polar mechanism and no outer sphere electron transfer processes. *Angew. Chem., Int. Ed. Engl. 34*, 1225−1227.
(38) Fukuzumi, S., Satoh, N., Okamoto, T., Yasui, K., Suenobu, T., Seko Y., Fujitsuka, M., and Ito, O. (2001) Change in spin state and enhancement of redox reactivity of photoexcited states of aromatic carbonyl compounds by complexation with metal ion salts acting as Lewis acids. Lewis acid catalyzed photoaddition of benzyltrimethylsilane and tetramethyltin via photoinduced electron transfer. *J. Am. Chem. Soc. 123*, 7756−7766.
(39) Mann, C. K., and Barnes, K. K. (1970) *Electrochemical Reactions in Non Aqueous Systems*, Mercel Dekker, New York.
(40) Sheldon, R. A. (1993) In *The Activation of Dioxygen and Homogeneous Catalytic Oxidation* (Barton, D. H. R., Martell, A. E., and Sawyer, D. T., Eds.) pp 9−30, Plenum Press, New York and London.
(41) Parshall, G. W., and Ittel, S. D. (1992) *Homogeneous Catalysis*, 2nd ed., Chapter 10, Wiley, New York.
(42) Sheldon, R., and Kochi, J. K. (1976) Metal catalyzed oxidations of organic compounds in the liquid phase: a mechanistic approach. *Adv. Catal. 25*, 272−413.
(43) Shilov, A. E. (1984) *Activation of Saturated Hydrocarbons by Transition Metal Complexes*, Chapter 4, D. Reidel Publishing Co., Dordrecht, The Netherlands.
(44) Bottcher, A., Birnbaum, E. R., Day, M. W., Gray, H. B., Grinstaff, M. W., and Labinger, J. A. (1997) How do electronegative substituents make metal complexes better catalysts for the oxidation of hydrocarbons by dioxygen? *J. Mol. Catal. A 117*, 229−242.
(45) Kochi, J. K. (1957) *Free Radicals in Solution*, John Wiley & Sons, New York.
(46) Kochi, J. K., Krusic, P. J., and Eaton, D. R. (1969) Homoallylic rearrangement and electron spin resonance of cyclopropylcarbinyl radicals. *J. Am. Chem. Soc. 91*, 1877−1879.
(47) Kochi, J. K., and Krusic, P. J. (1968) Electron spin resonance of aliphatic hydrocarbon radicals in solution. *J. Am. Chem. Soc. 90*, 7155−7157.
(48) Kochi, J. K., and Krusic, P. J. (1969) Electron spin resonance of organosilyl radicals in solution. *J. Am. Chem. Soc. 91*, 3938−3940.
(49) Kochi, J. K., and Krusic, P. J. (1969) Electron spin resonance studies of homolytic substitution reactions. Oraganoboron, aluminum, and gallium compounds. *J. Am. Chem. Soc. 91*, 3942−3944.
(50) Kochi, J. K., and Krusic, P. J. (1969) Displacement of alkyl groups from organophosphorus compounds studied by electron spin resonance. *J. Am. Chem. Soc. 91*, 3944−3946.
(51) Howard, J. A., and Furimsky, E. (1974) Electron spin resonance study on the *tert* butylsulfinyl radical. *Can. J. Chem. 52*, 555−556.
(52) Fukuzumi, S., and Ono, Y. (1977) Decay kinetics of cumylperoxyl radical produced by the decomposition of cumene hydroperoxide. *J. Chem. Soc., Perkin Trans. 2*, 622−625.
(53) Fukuzumi, S., and Ono, Y. (1977) Electron spin resonance and kinetic studies on the liquid phase autoxidation of cumene with lead dioxide. *J. Chem. Soc., Perkin Trans. 2*, 784−788.
(54) Watanabe, T., Yuki, S., Egawa, M., and Nishi, H. (1994) Protective effects of MCI 186 on cerebral ischemia: possible involvement of free radical scavenging and antioxidant actions. *J. Pharmacol. Exp. Ther. 268*, 1597−1604.
(55) Yamamoto, T., Yuki, S., Watanabe, T., Mitsuya, M., and Saito, K. (1997) Delayed neuron death prevented by inhibition of increased hydroxyl radical formation in a transient cerebral ischemia. *Brain Res. 762*, 240−242.
(56) Okatani, Y., Wakatsuki, A., Enzan, H., and Miyahara, Y. (2003) Edaravone protects against ischemia/reperfusion induced oxidative damage to mitochondria in rat liver. *Eur. J. Pharmacol. 465*, 163−170.
(57) Thomas, J. P., Tutsch, K. D., Cleary, J. F., Bailey, H. H., Arzoomanian, R., Alberti, D., Simon, K., Feierabend, C., Binger, K., Marnocha, R., Dresen, A., and Wilding, G. (2002) Phase I clinical and pharmacokinetic trial of the cyclin dependent kinase inhibitor flavopiridol. *Cancer Chemother. Pharmacol. 50*, 465−472.
(58) Kouriukis, C. T., Belch, A., Crump, M., Eisenhauer, E., Gascoyne, R. D., Meyer, R., Lohmann, R., Lopez, P., Powers, J., Turner, R., and Connors, J. M. (2003) Flavopiridol in untreated of relapsed mantle cell lymphoma: results of a phase II study of the National Cancer Institute of Canada Clinical Trials Group. *J. Clin. Oncol. 21*, 1740−1745.
(59) Senderowicz, A. M. (2002) Cyclin dependent kinases as new targets for the prevention and treatment of cancer. *Hematol. Oncol. Clin. North Am. 16*, 1229−1253.
(60) Ngnokam, D., Massiot, G., Nuzillard, J. M., and Tsamo, E. (1994) (+) 7′,7′ Dimethyl 5 hydroxy 2R,3S trans pubeschin from *Entandrophragma cylindricum*. *Phytochemistry 37*, 529−531.
(61) Davis, K. J. A. (1996) Oxidative stress: The paradox of aerobic life. *Biochem. Soc. Symp. 61*, 1−31.
(62) Nakanishi, I., Fukuhara, K., Shimada, T., Ohkubo, K., Iizuka, Y., Inami, K., Mochizuki, M., Urano, S., Itoh, S., Miyata, N., and Fukuzumi, S. (2002) Effects of magnesium ion on kinetic stability and spin distribution of phenoxyl radical derived from a vitamin E analogues: mechanistic insight into antioxidative hydrogen transfer reaction of vitamin E. *J. Chem. Soc., Perkin Trans. 2*, 1520−1524.
(63) Fukuzumi, S., Shimoosako, K., Suenobu, T., and Watanabe, Y. (2003) Mechanism of hydrogen , oxygen , and electron transfer reactions of cumylperoxyl radical. *J. Am. Chem. Soc. 125*, 9074−9082.
(64) Itoh, S., Kumei, H., Nagatomo, S., Kitagawa, T., and Fukuzumi, S. (2001) Effects of metal ions on physicochemical properties and redox reactivity of phenolates and phenoxyl radicals: mechanistic insight into hydrogen atom abstraction by phenoxyl radical metal complexes. *J. Am. Chem. Soc. 123*, 2165−2175.
(65) Itoh, S., Maruta, J., and Fukuzumi, S. (1996) Addition cyclization reaction of nitroalkane anions with *o*-quinone derivatives via electron transfer in the charge transfer complexes. *J. Chem. Soc., Perkin Trans. 2*, 1429−1433.
(66) Boozer, C. E., and Hammond, G. S. (1954) Molecular complex formation in free radical reactions. *J. Am. Chem. Soc. 76*, 3861−3862.
(67) Boozer, C. E., Hammond, G. S., Hamilton, C. E., and Sen, J. N. (1955) Air oxidation of hydrocarbons. II. The stoichiometry and fate of inhibitors in benzene and chlorobenzene. *J. Am. Chem. Soc. 77*, 3233−3237.

TX034134C

Chem. Res. Toxicol. **2004,** *17,* 1750−1756

Oxidative DNA Damage Induced by Carcinogenic Dinitropyrenes in the Presence of P450 Reductase

Mariko Murata,[†] Shiho Ohnishi,[†] Kazuharu Seike,[†] Kiyoshi Fukuhara,[‡] Naoki Miyata,[§] and Shosuke Kawanishi*,[†]

Department of Environmental and Molecular Medicine, Mie University School of Medicine, 2-174, Edobashi, Tsu, Mie 514-8507, Japan, National Institute of Health Science, 1-18-1, Kamiyouga Setagaya-ku, Tokyo 158-8501, Japan, and Department of Graduate School of Pharmaceutical Sciences, Nagoya City University, 3-1 Tanabe-dori, Mizuho-ku, Nagoya, Aichi 467-8603, Japan

Received September 2, 2004

Nitropyrenes are widespread in the environment due to mainly diesel engine emissions. Dinitropyrenes (DNPs), especially 1,8-dinitropyrene (1,8-DNP) and 1,6-dinitropyrene (1,6-DNP), are much more potent mutagens than other nitropyrenes. The carcinogenicity of 1,8-DNP and 1,6-DNP is stronger than 1,3-dinitropyrene (1,3-DNP). It is considered that adduct formation after metabolic activation plays an important role in the expression of carcinogenicity of nitropyrenes. However, Djuric et al. [(1993) *Cancer Lett.*] reported that oxidative DNA damage was also found as well as adduct formation in rats treated with 1,6-DNP. We investigated oxidative DNA damage by DNPs in the presence of NAD(P)H-cytochrome P450 reductase using ^{32}P-5′-end-labeled DNA. After P450 reductase treatment, DNPs induced Cu(II)-mediated DNA damage in the presence of NAD(P)H. The intensity of DNA damage by 1,8-DNP or 1,6-DNP was stronger than 1,3-DNP. We also examined synthetic 1-nitro-8-nitrosopyrene (1,8-NNOP) and 1-nitro-6-nitrosopyrene (1,6-NNOP) as one of the metabolites of 1,8-DNP and 1,6-DNP, respectively, to find that 1,8-NNOP and 1,6-NNOP induced Cu(II)-mediated DNA damage in the presence of NAD(P)H but untreated DNPs did not. In both cases of P450 reductase-treated DNPs and NNOPs, catalase and a Cu(I) specific chelator attenuated DNA damage, indicating the involvement of H_2O_2 and Cu(I). Using a Clarke oxygen electrode, oxygen consumption by the reaction of NNOPs with NAD(P)H and Cu(II) was measured to find that NNOP was nonenzymatically reduced by NAD(P)H and that the addition of Cu(II) promoted the redox cycle. Therefore, these results suggest that DNPs are enzymatically reduced to NNOPs via nitro radical anion and that NNOPs are further reduced nonenzymatically by NAD(P)H. Subsequently, autoxidation of nitro radical anion and the reduced form of NNOP occurs, resulting in O_2^- generation and DNA damage. We conclude that oxidative DNA damage in addition to DNA adduct formation may play important roles in the carcinogenesis of DNPs via their metabolites.

Introduction

Nitropolycyclic aromatic hydrocarbons including nitropyrenes (NPs) are widespread in the environment due to mainly diesel engine emissions (*1*, *2*). NPs are strongly mutagenic in the bacterial mutation assay (Ames test) and human cell mutagenicity assay (*3*, *4*). Dinitropyrenes (DNPs),[1] especially 1,8-dinitropyrene (1,8-DNP) and 1,6-dinitropyrene (1,6-DNP), are much more potent mutagens than other nitropyrenes. DNPs induced lung cancer and leukemia in rodents. An epidemiological study demonstrated that significant positive trends in lung cancer risk were observed with increasing cumulative exposure of diesel exhaust in male truck drivers (*5*). The International Agency for Research on Cancer (IARC) has assessed that 1,8-DNP and 1,6-DNP have been possibly carcinogenic to humans (group 2B), whereas 1,3-dinitropyrene (1,3-DNP) has not been classifiable as to its carcinogenicity to humans (group 3) (*1*).

Chemical mutagenesis is strongly affected by metabolic activation. Cellular nitroreductase and *O*-acetyltransferase activities have been shown to markedly influence the genotoxic activity of nitro-aromatic compounds (*6*). DNA adduct formation after metabolic activation has been considered to be a major causal factor of carcinogenesis by DNPs. DNPs undergo nitroreduction to *N*-hydroxy arylamines that bind to DNA directly or after *O*-esterification (*1*). DNP adducts are identified as *N*-(deoxyguanosin-8-yl)amino-nitropyrene (dG-C8-1,6-ANP and dG-C8-1,8-ANP), leading to mutation and carcinogenesis (*1*, *7*). On the other hand, Djuric et al. found not only DNA adducts but also oxidative DNA damage in rats

* To whom correspondence should be addressed. Tel/Fax: +81-59-231-5011. E-mail: kawanisi@doc.medic.mie-u.ac.jp.
† Mie University School of Medicine.
‡ National Institute of Health Science.
§ Nagoya City University.

[1] Abbreviations: DNPs, dinitropyrenes; 1,3-DNP, 1,3-dinitropyrene; 1,6-DNP, 1,6-dinitropyrene; 1,8-DNP, 1,8-dinitropyrene; NNOPs, nitronitrosopyrenes; 1,6-NNOP, 1-nitro-6-nitrosopyrene; 1,8-NNOP, 1-nitro-8-nitrosopyrene; 8-oxodG, 8-oxo-7,8-dihydro-2′-deoxyguanosine; NAD(P)H, β-nicotinamide adenine dinucleotide (phosphate) (reduced form); P450 reductase, NAD(P)H-cytochrome P450 reductase; O_2^-, superoxide; ECD, electrochemical detector; DTPA, diethylenetriamine-*N*,*N*,*N*′,*N*″,*N*″-pentaacetic acid; SOD, superoxide dismutase.

10.1021/tx0497550 CCC: $27.50
Published on Web 11/24/2004

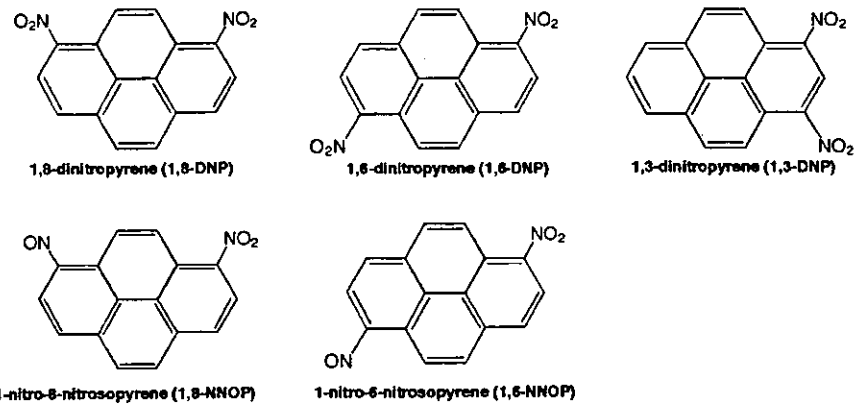

Figure 1. Chemical structures of DNPs and their metabolites used in this study.

treated with 1,6-DNP (*8*). Furthermore, we previously revealed the role of a nitroso derivative of 1-nitropyrene on causing oxidative DNA damage (*9*). It has been reported that nitro-nitroso derivatives are metabolic intermediates of DNPs during metabolic activation, which are more mutagenic than their parent DNPs (*10*). These indicate that oxidative DNA damage by DNPs after metabolic activation plays a role in carcinogenesis.

In this study, we investigated oxidative DNA damage induced by DNPs in the presence of NAD(P)H-cytochrome P450 reductase (P450 reductase), using ^{32}P-5′-end-labeled DNA fragments obtained from the human *p53* and *p16* tumor suppressor genes and the c-Ha-*ras*-1 protooncogene. We also examined synthetic nitro-nitrosopyrenes (NNOP), 1-nitro-8-nitrosopyrene (1,8-NNOP), and 1-nitro-6-nitrosopyrene (1,6-NNOP) as nitroso metabolites of DNP. The chemical structures of DNPs and synthetic NNOPs used in this study are shown in Figure 1. We also analyzed 8-oxo-7,8-dihydro-2′-deoxyguanosine (8-oxodG) formation in calf thymus DNA.

Materials and Methods

Materials. 1,6-NNOP and 1,8-NNOP were synthesized by oxidation of 1-nitro-6-aminopyrene and 1-nitro-8-aminopyrene, respectively, according to the method by the reference (*11*). The nitroaminopyrene used in the synthesis was carried out until none of the undesired isomer could be detected by ^{1}H NMR spectroscopy. To a solution of the purified aminonitropyrene dissolved in CH_3Cl, a solution of *m*-CPBA in CH_3Cl was added dropwise over 20 min and the reaction was carried out at 5 °C for 4 h. The mixture was washed with saturated $NaHCO_3$ and brine, and the organic phase was dried over anhydrous Na_2SO_4. Following evaporation in vacuo, the product was obtained by column chromatography on silica gel using *n*-hexanes−ethyl acetate as the eluent and further recrystallization from *n*-hexanes−ethyl acetate to produce light orange crystals. The purity of each compound was >99% as assessed by ^{1}H NMR spectroscopy.

1. 1,6-NNOP. ^{1}H NMR (400 MHz DMSO-d_6): δ 7.04 (1H, d, J = 8.8 Hz), 8.49 (1H, d, J = 8.8 Hz), 8.64 (1H, d, J = 9.2 Hz), 8.84 (1H, d, J = 8.4 Hz), 8.92 (1H, d, J = 8.4 Hz), 8.97 (1H, d, J = 9.6 Hz), 9.00 (1H, d, J = 9.2 Hz), 10.42 (1H, d, J = 9.6 Hz), mp 244 °C (decomp.) [lit. (*11*) >233 °C (decomp.)].

2. 1,8-NNOP. ^{1}H NMR (400 MHz DMSO-d_6): δ 7.03 (1H, d, J = 8.4 Hz), 8.49 (1H, d, J = 8.4 Hz), 8.55 (1H, d, J = 8.8 Hz), 8.71 (1H, d, J = 8.8 Hz), 8.75 (1H, d, J = 8.8 Hz), 8.92 (1H, d, J = 8.8 Hz), 9.21 (1H, d, J = 9.6 Hz), 10.45 (1H, d, J = 9.6 Hz), mp 268 °C (decomp.) [lit. (*11*) >245 °C (decomp.)].

Restriction enzymes (*Hind* III, *Sty* I, *Apa* I, *Ava* I, and *Xba* I) and T_4 polynucleotide kinase were purchased from New England Biolabs (Beverly, MA). [γ-^{32}P]ATP (222 TBq/mmol) was obtained from New England Nuclear. Alkaline phosphatase from calf intestine was purchased from Roche Molecular Biochemicals (Mannheim, Germany). 1,8-DNP, 1,6-DNP, and 1,3-DNP were purchased from Aldrich Chemical Co. (Milwaukee, IL; the purities were 98, 98, and 99%, respectively). P450 reductase from rat microsome was a kind gift from Prof. Y. Kumagai (Tsukuba University). Piperidine was purchased from Wako Chemical Industries Ltd. (Osaka, Japan). Copper(II) chloride dihydrate was purchased from Nacalai Tesque, Inc. (Kyoto, Japan). Diethylenetriamine-*N*,*N*,*N*′,*N*″,*N*″-pentaacetic acid (DTPA) and bathocuproinedisulfonic acid were purchased from Dojin Chemicals Co. (Kumamoto, Japan). Calf thymus DNA, superoxide dismutase (SOD) (3000 units/mg from bovine erythrocytes), and catalase (45000 units/mg from bovine liver) were purchased from Sigma Chemical Co. (St. Louis, MO). Nuclease P_1 (400 units/mg) was purchased from Yamasa Shoyu Co. (Chiba, Japan).

Preparation of ^{32}P-5′-End-Labeled DNA Fragments Obtained from the *p53* Gene, the *p16* Gene, and the c-Ha-*ras*-1 Gene. DNA fragments were obtained from the human *p53* and *p16* tumor suppressor gene (*12*, *13*) and the c-Ha-*ras*-1 protooncogene (*14*). A singly ^{32}P-5′-end-labeled double-stranded 443 bp fragment (*Apa* I 14179-*Eco* RI* 14621) from the *p53* gene was prepared from the pUC18 plasmid according to a method described previously (*15*). A singly labeled 328 bp fragment (*Eco*RI*5841-*Mro*I 6168) of the *p16* gene was prepared from pGEM-T Easy Vector (Promega Corporation) as described previously (*16*). A 261 bp fragment (*Ava* I* 1645-*Xba* I 1905) and a 341 bp fragment (*Xba*I 1906-*Ava*I* 2246) from the c-Ha-*ras*-1 gene were prepared from plasmid pbcNI, which carries a 6.6 kb *Bam*H I chromosomal DNA restriction fragment as described previously (*17*). The asterisk indicates ^{32}P labeling.

Detection of DNA Damage. A standard reaction mixture (in a microtube; 1.5 mL) contained $CuCl_2$, NAD(P)H, NNOP, ^{32}P-5′-end-labeled double-stranded DNA fragments, and calf thymus DNA in 200 μL of 10 mM sodium phosphate buffer (pH 7.8). For nitroreduction, DNP, 100 μM NADPH, and P450 reductase were preincubated at 25 °C for 30 min in 20 mM potassium phosphate buffer (pH 7.4). After the preincubation, ^{32}P-labeled DNA fragments, calf thymus DNA, and $CuCl_2$ were added to the mixtures (total 200 μL), followed by the incubation. After incubation at 37 °C for 1 h, DNA fragments were treated in 10% (v/v) piperidine at 90 °C for 20 min or treated with 6 units of Fpg protein in reaction buffer [10 mM HEPES−KOH (pH 7.4), 100 mM KCl, 10 mM EDTA, and 0.1 mg/mL BSA] at 37 °C for 2 h, as described previously (*18*). The treated DNA fragments were electrophoresed on an 8% polyacrylamide/8 M urea gel, and an autoradiogram was obtained by exposing X-ray film to the gel. To make the dose of DNA constant, we used calf thymus DNA (20−50 μM) at an excessive dose as compared with ^{32}P-labeled DNA (less than pM) that can be negligible, because the required dose of ^{32}P-labeled DNA, for detection of DNA damage, varies according to the decaying radioactivity (^{32}P; $T_{1/2}$ = 14 days). The preferred cleavage sites were determined by direct comparison of the positions of the oligonucleotides with those produced by the chemical reactions of the Maxam−Gilbert

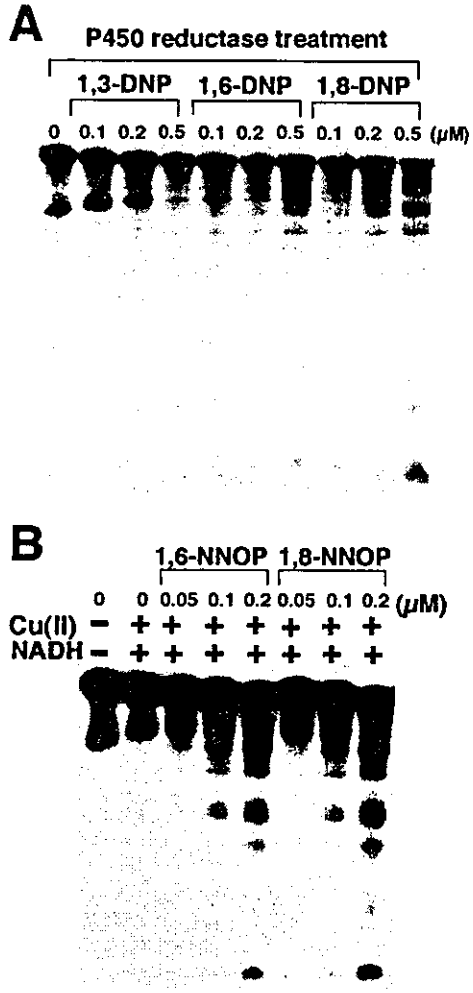

Figure 2. Autoradiogram of ^{32}P-labeled DNA fragment treated with DNPs and their nitro-nitroso derivatives. (A) The reaction mixtures containing the indicated concentrations of DNPs, 100 μM NADPH, and 2.1 μg/mL P450 reductase were preincubated at 25 °C for 30 min in potassium phosphate buffer (pH 7.4). After preincubation, a ^{32}P-5′-end-labeled 328 bp DNA fragment, calf thymus DNA (20 μM/base), and 20 μM $CuCl_2$ were added to the mixtures. (B) The reaction mixture contained a ^{32}P-5′-end-labeled 341 bp DNA fragment, calf thymus DNA (50 μM/base), the indicated concentrations of 1,8-NNOP or 1,6-NNOP, 100 μM NADH, and 20 μM $CuCl_2$ in sodium phosphate buffer (pH 7.8). The reaction mixtures were incubated at 37 °C for 1 h, followed by piperidine treatment, as described in the Materials and Methods. The DNA fragments were electrophoresed on an 8% polyacrylamide/8 M urea gel, and an autoradiogram was obtained by exposing an X-ray film to the gel.

procedure (*19*) using a DNA sequencing system (LKB 2010 Macrophor). A laser densitometer (LKB 2222 UltroScan XL) was used for the measurement of the relative amounts of oligonucleotides from the treated DNA fragments.

Analysis of 8-OxodG Formation by DNPs and NNOPs. The calf thymus DNA fragment was incubated with NNOP or treated DNP, NAD(P)H, and $CuCl_2$. After ethanol precipitation, DNA was digested to its component nucleosides with nuclease P_1 and calf intestine phosphatase and analyzed by HPLC-electrochemical detector (ECD), as described previously (*20*).

Measurement of Oxygen Consumption. Oxygen consumption by the reaction of NNOPs with NADH and $CuCl_2$ was measured using a Clarke oxygen electrode (Electronic Stirrer model 300, Rank Brothers Ltd., Bottisham Cambridge, United Kingdom). The reactions were performed in a mixture containing NNOP, NADH, and $CuCl_2$ in 2 mL of 10 mM phosphate buffer (pH 7.8) containing 2.5 μM DTPA at 37 °C. Catalase was added in order to detect H_2O_2 generation due to oxygen consumption.

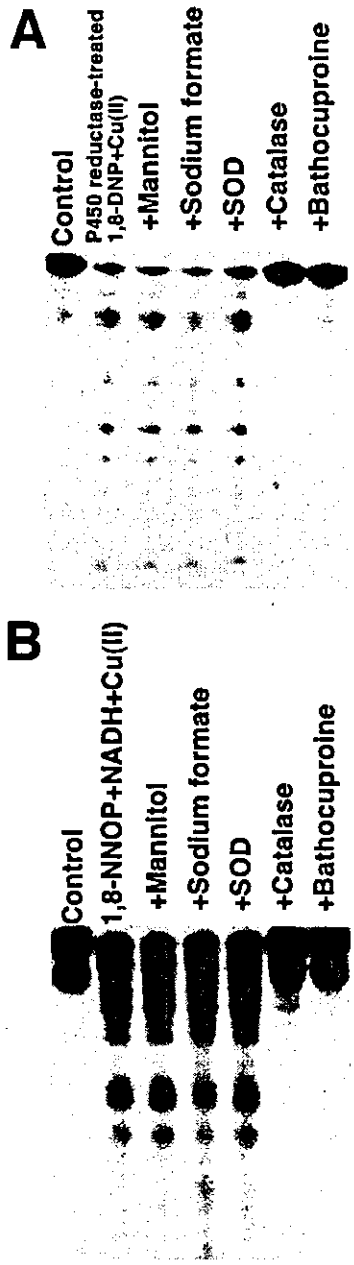

Figure 3. Effects of scavengers and bathocuproine on Cu(II)/NAD(P)H-mediated DNA damage induced by P450 reductase-catalyzed 1,8-DNP and 1,8-NNOP. (A) The reaction mixtures containing 0.5 μM 1,8-DNP, 100 μM NADPH, and 2.1 μg/mL P450 reductase were preincubated at 25 °C for 30 min in potassium phosphate buffer (pH 7.4). After preincubation, a ^{32}P-5′-end-labeled 309 bp DNA fragment, calf thymus DNA (20 μM/base), 20 μM $CuCl_2$, and a scavenger were added to the mixtures. (B) The reaction mixture contained a ^{32}P-5′-end-labeled 261 bp DNA fragment, calf thymus DNA (20 μM/base), 0.2 μM 1,8-NNOP, 20 μM $CuCl_2$, and a scavenger in sodium phosphate buffer (pH 7.8). The reaction mixtures were incubated at 37 °C for 1 h, followed by piperidine treatment. The DNA fragments were analyzed as described in the legend to Figure 2. The concentrations of scavengers and bathocuproine were as follows: 0.1 M mannitol, 0.1 M sodium formate, 30 units of SOD, 30 units of catalase, and 50 μM bathocuproine.

Results

Damage to ^{32}P-Labeled DNA. Figure 2 shows an autoradiogram of a DNA fragment treated with DNPs and NNOPs. Oligonucleotides were detected on the autoradiogram as a result of DNA damage. DNPs did not cause DNA damage in the presence of NAD(P)H and Cu-

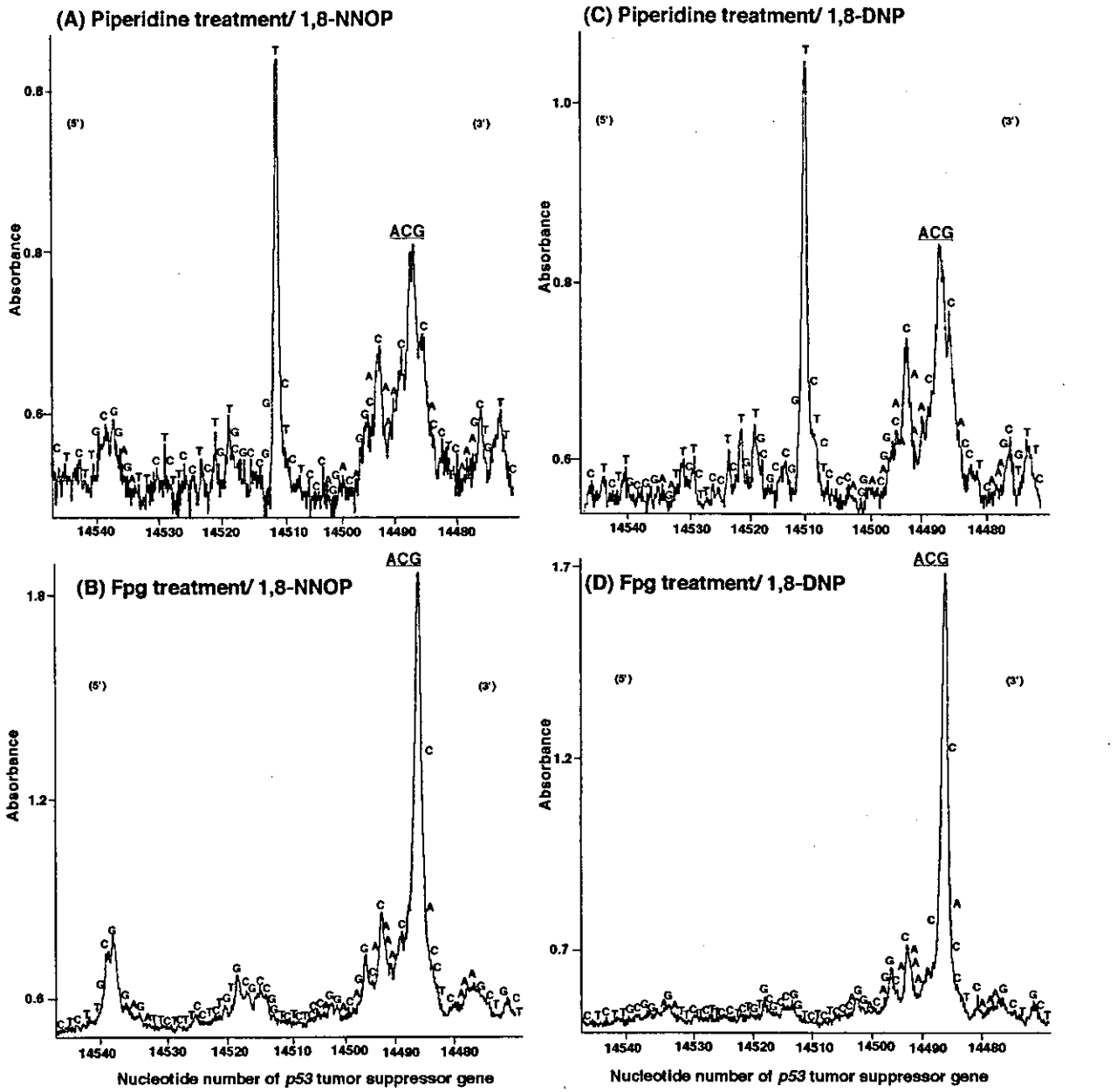

Figure 4. Site specificity of DNA cleavage induced by P450 reductase-treated 1,8-DNP and 1,8-NNOP in the presence of NADPH and Cu(II). The reaction mixtures containing 0.5 μM 1,8-NNOP (A, B) or 0.5 μM 1,8-DNP (C, D), 100 μM NADPH with (C, D) or without (A, B) 2.1 μg/mL P450 reductase were preincubated at 25 °C for 30 min in potassium phosphate buffer (pH 7.4). After preincubation, a ^{32}P-5′-end-labeled 443 bp DNA fragment, calf thymus DNA (20 μM/base), and 20 μM $CuCl_2$ were added to the mixtures. The reaction mixtures were incubated at 37 °C for 1 h, followed by piperidine treatment (A, C) or Fpg treatment (B, D). The horizontal axis shows the nucleotide number of the human *p53* tumor suppressor gene, and underscoring shows the complementary sequence to codon 273 (nucleotides 14486−14488).

(II) (data not shown). When P450 reductase was added, DNPs induced Cu(II)-mediated DNA damage (Figure 2A). 1,8-DNP and 1,6-DNP induced DNA damage more efficiently than 1,3-DNP did.

NNOPs, nitro-reduced metabolites of DNPs, were synthesized in order to compare with parent DNP. 1,8-NNOP and 1,6-NNOP induced DNA damage without P450 reductase (Figure 2B). These NNOPs induced DNA damage in the presence of NAD(P)H and Cu(II). In the absence of either NAD(P)H or Cu(II), NNOPs did not cause DNA damage. NNOPs alone did not cause DNA damage (data not shown).

Effects of Scavengers and Bathocuproine on DNA Damage. The effects of scavengers and bathocuproine on DNA damage by 1,8-DNP with P450 reductase are shown in Figure 3A. Mannitol and sodium formate, typical ·OH scavengers, did not inhibit DNA damage. Catalase and bathocuproine, a Cu(I) specific chelator, inhibited DNA damage, whereas SOD did not reduce the amount of DNA damage. Similar inhibitory effects were observed in the cases of 1,8-NNOP (Figure 3B). When 1,6-isomers were used instead of 1,8-isomers, similar results were obtained (data not shown).

Site Specificity of DNA Damage by 1,8-DNP with P450 Reductase and 1,8-NNOP. An autoradiogram was scanned with a laser densitometer to measure the relative intensities of DNA cleavage products from the human *p53* tumor suppressor gene. 1,8-NNOP and P450 reductase-treated 1,8-DNP induced piperidine labile sites relatively at thymine and cytosine residues in the pres-

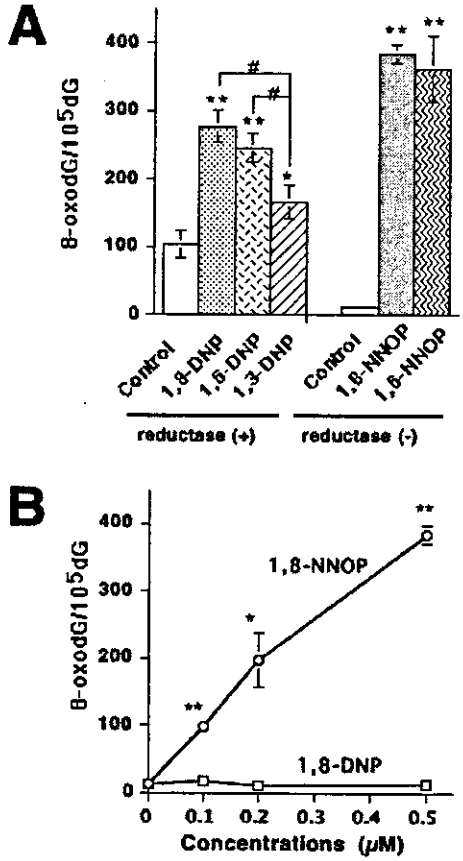

Figure 5. Formation of 8-oxodG by P450 reductase-treated DNPs and NNOPs in the presence of NADPH and Cu(II). For DNPs, the reaction mixtures containing 0.5 μM DNPs, 100 μM NADPH, and 2.1 μg/mL P450 reductase were preincubated at 25 °C for 30 min in potassium phosphate buffer (pH 7.4). After preincubation, calf thymus DNA (100 μM/base) and 20 μM $CuCl_2$ were added to the mixtures, followed by the incubation of 37 °C for 1 h. For NNOPs, the reaction mixtures containing calf thymus DNA (100 μM/base), 0.5 μM NNOPs (A), or the indicated concentrations of NNOPs (B), 100 μM NADPH, and 20 μM $CuCl_2$ were incubated at 37 °C for 1 h in potassium phosphate buffer (pH 7.4). After ethanol precipitation, DNA was enzymatically digested to individual nucleosides, and the 8-oxodG content was measured by HPLC-ECD as described in the Materials and Methods. Results are expressed as means and SD of values obtained from three independent experiments. Symbols indicate a significant difference as compared with control (*$P < 0.05$; **$P < 0.01$) and significant difference among DNPs (#$P < 0.05$) by *t*-test.

ence of Cu(II) and NAD(P)H (Figure 4A,C). With Fpg treatment, DNA cleavage occurred mainly at guanine and cytosine residues (Figure 4B,D). 1,8-NNOP and 1,8-DNP caused piperidine labile and Fpg sensitive lesions at CG in the 5′-ACG-3′ sequence, a well-known hotspot (*21*) of the *p53* gene.

Formation of 8-OxodG in Calf Thymus DNA. Using HPLC-ECD, we measured the 8-oxodG content of calf thymus DNA incubated with NNOPs and P450 reductase-treated DNPs (Figure 5A). P450 reductase-treated DNPs significantly increased the amount of 8-oxodG as compared with the control (1,8-DNP, $P < 0.01$; 1,6-DNP, $P < 0.01$; 1,3-DNP, $P < 0.05$). The order of 8-oxodG content was as follows: 1,8-DNP, 1,6-DNP > 1,3-DNP > control. 1,8-DNP and 1,6-DNP induced 8-oxodG formation more efficiently than 1,3-DNP ($P < 0.01$ and $P < 0.05$, respectively). There was no significant difference in 8-oxodG formation between 1,8-DNP and 1,6-DNP, after P450 reductase treatment. 1,8-NNOP and

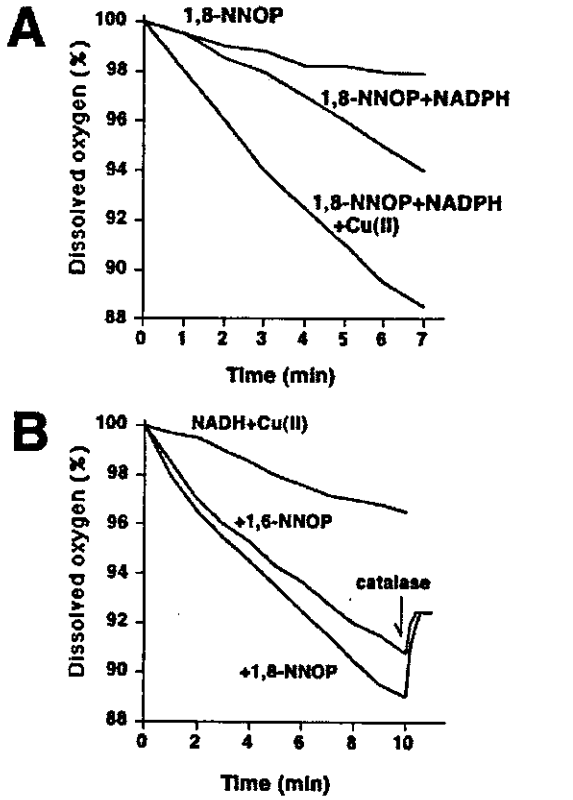

Figure 6. Oxygen consumption by the interaction of NNOPs with NAD(P)H and Cu(II). (A) Reaction mixtures contain 100 μM 1,8-NNOP, 2 mM NADPH, and/or 100 μM $CuCl_2$ in 2 mL of 10 mM phosphate buffer (pH 7.4) at 37 °C. (B) Reaction mixtures contain 100 μM NNOP, 2 mM NADH, and/or 100 μM $CuCl_2$ in 2 mL of 10 mM phosphate buffer (pH 7.8) at 37 °C. To detect H_2O_2 generation during oxygen consumption, 100 units of catalase were added at 10 min (indicated by an arrow).

1,6-NNOP without reductase significantly induced 8-oxodG formation in the presence of Cu(II) and NAD(P)H (Figure 5A).

1,8-NNOP significantly induced Cu(II)/NAD(P)H-mediated 8-oxodG formation in a dose-dependent manner (Figure 5B). 1,8-DNP induced no significant increase of 8-oxodG formation without P450 reductase. In the case of 1,6-NNOP, similar results were obtained (data not shown).

Oxygen Consumption during the Reaction of NNOP in the Presence of NADH and Cu(II). Oxygen consumption was observed in the reaction of 1,8-NNOP with NADH and Cu(II) (Figure 6). In the case of 1,8-NNOP alone, a little amount of oxygen consumption was observed. The addition of NADH increased oxygen consumption to some extent. In the reaction of 1,8-NNOP with NADH and Cu(II), a large amount of oxygen was consumed (Figure 6A). Figure 6B shows oxygen consumption by 1,8-NNOP and 1,6-NNOP in the presence of NADH and Cu(II). In the reaction of NADH and Cu(II), a little amount of oxygen consumption was observed. 1,8-NNOP induced oxygen consumption a little more efficiently than 1,6-NNOP. The addition of catalase increased dissolved oxygen, suggesting the generation of H_2O_2 that was decomposed by catalase to yield oxygen.

Discussion

The present study demonstrated the abilities of oxidative DNA damage by DNPs and their nitroso metabolites. NNOPs caused oxidative DNA damage in the presence

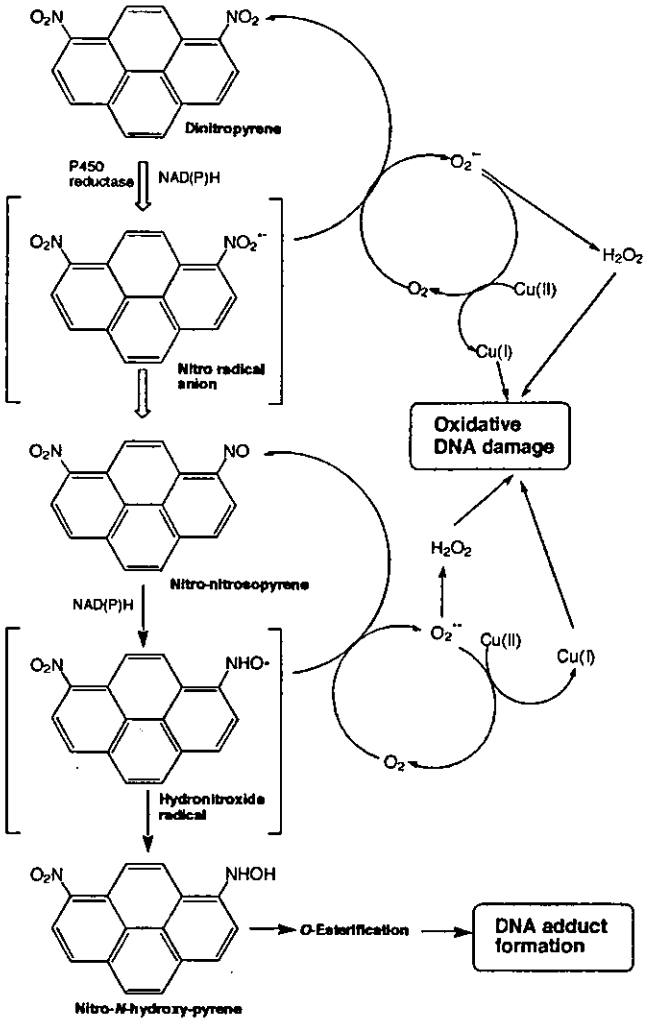

Figure 7. Proposed mechanism of oxidative DNA damage induced by DNPs in the presence of P450 reductase, NAD(P)H, and Cu(II).

of NAD(P)H and Cu(II), but DNPs did not. After the treatment of P450 reductase, DNPs, especially 1,8-DNP and 1,6-DNP, induced Cu(II)-mediated DNA damage. Both catalase and bathocuproine were found to reduce the DNA damage, indicating the involvement of H_2O_2 and Cu(I). These results suggested that NNOP was nonenzymatically reduced by NAD(P)H and autoxidized again by reacting with molecular oxygen to generate superoxide (O_2^-), and the addition of Cu(II) promoted the redox cycle. On the basis of these results, a possible mechanism could be proposed as follows (Figure 7). P450 reductase catalyzes one or more electron reduction of DNP to nitro radical anion and/or further reduced forms. Autoxidation of the reduced form yields O_2^-. NNOP can be reduced by an endogenous reductant NAD(P)H, to a reactive intermediate, which is probably a hydronitroxide radical. Autoxidation of this intermediate to NNOP occurs, coupled with the generation of O_2^-. O_2^- is dismutated to H_2O_2 and reduces Cu(II) to Cu(I). H_2O_2, in turn, interacts with Cu(I) to form a reactive oxygen species, which causes DNA damage. Study using a Clarke oxygen electrode confirmed oxygen consumption by the reaction of NNOPs with NADH and Cu(II). The addition of catalase increased the level of dissolved oxygen by the decomposition of H_2O_2 to oxygen. It is suggested that the dissolved oxygen in the reaction mixture is converted to O_2^- by the reduced forms of DNPs and NNOPs. Collectively, NNOP and P450 reductase-treated DNP significantly induce DNA damage including 8-oxodG formation through NAD(P)H-dependent redox cycles. The amounts of 8-oxodG induced by DNPs and NNOPs (0.5 μM) through the redox cycles corresponded to those induced by 30–60 μM H_2O_2 in the presence of Cu(II). The concentration of NAD(P)H in certain tissue has been estimated to be as high as 100–200 μM (*22*). The biological importance of NADH and NADPH as nuclear reductants (*23*) has been demonstrated before (*24, 25*). P450 reductase and other enzymes with nitroreduction activity, such as NAD(P)H:quinone oxidoreductase and xanthine oxidase (*26, 27*), may participate in activation of DNPs in vivo.

We showed that DNPs with P450 reductase treatment induced DNA damage including 8-oxodG formation in the intensity of 1,8-DNP, 1,6-DNP > 1,3-DNP. Consistently, among three DNP isomers, 1,3-DNP appears to be a weaker carcinogen (*1*) and mutagen (*3, 4*). 1,6-DNP and 1,8-DNP are more efficiently nitro-reduced by liver cytosol and microsomes than 1,3-DNP (*28*). Similarly, Djuric (*29*) demonstrated that NADPH-mediated reduction of 1,3-NNOP to intermediates was slower than that of 1,6-NNOP. These differences in rates of enzyme efficacy to DNPs are considered to be one factor contributing to the differences of DNA damaging ability. This may explain the lower carcinogenic potential of 1,3-DNP as compared to 1,6-DNP and 1,8-DNP. Our results have suggested that DNPs are enzymatically reduced to NNOPs and are subsequently followed by the autoxidation of nitro radical anion and NAD(P)H-dependent reduction of NNOPs, resulting in Cu(II)-dependent redox cycle formation and DNA damage. This oxidative DNA damage may be supported by the report of Djuric et al. showing not only DNA adducts but also oxidative DNA damage in rats treated with 1,6-DNP (*8*).

Kohara et al. (*30*) showed that DNPs treatment increased the incidence of G → T transversions in mice. In this study, P450 reductase-treated DNPs induced Fpg sensitive sites preferentially at guanine residues and increased 8-oxodG formation. Shibutani et al. (*31*) have reported that 8-oxodG causes DNA misreplication, which can lead to mutation, particularly G → T substitutions. In addition, the bacterial mutation assay (*32*) revealed that DNPs exerted frequent base substitution mutations at cytosine residues. We demonstrated that NNOPs and P450 reductase-treated DNPs induced DNA cleavage sites preferentially at cytosine residues. Furthermore, piperidine and Fpg treatment detected cytosine and guanine damage of the ACG sequence complementary to codon 273, a well-known hotspot (*21*) of the *p53* gene. The occurrence of mutational hotspots may be partly explained by our observations. It is concluded that oxidative DNA damage, in addition to DNA adduct formation, may play important roles in the carcinogenesis of DNPs via metabolic activation on nitro group.

Acknowledgment. This work was supported by Grants-in-Aid for Scientific Research from the Ministry of Education, Science, Sports and Culture of Japan.

References

(1) IARC (1989) Diesel and gasoline engine exhausts and some nitroarenes. *IARC Monographs on the Evaluation of the Carcinogenic Risks to Humans*, Vol. 46, pp 1–373, IARC Press, Lyon.
(2) Watanabe, T., Hasei, T., Takahashi, Y., Otake, S., Murahashi, T., Takamura, T., Hirayama, T., and Wakabayashi, K. (2003) Mutagenic activity and quantification of nitroarenes in surface soil in the Kinki region of Japan. *Mutat Res. 538*, 121–131.

(3) Busby, W. F., Jr., Penman, B. W., and Crespi, C. L. (1994) Human cell mutagenicity of mono- and dinitropyrenes in metabolically competent MCL-5 cells. *Mutat Res. 322*, 233–242.
(4) Busby, W. F., Jr., Smith, H., Bishop, W. W., and Thilly, W. G. (1994) Mutagenicity of mono- and dinitropyrenes in the *Salmonella typhimurium* TM677 forward mutation assay. *Mutat. Res. 322*, 221–232.
(5) Steenland, K., Deddens, J., and Stayner, L. (1998) Diesel exhaust and lung cancer in the trucking industry: Exposure-response analyses and risk assessment. *Am. J. Ind. Med. 34*, 220–228.
(6) Carroll, C. C., Warnakulasuriyarachchi, D., Nokhbeh, M. R., and Lambert, I. B. (2002) *Salmonella typhimurium* mutagenicity tester strains that overexpress oxygen-insensitive nitroreductases nfsA and nfsB. *Mutat. Res. 501*, 79–98.
(7) Hilario, P., Yan, S., Hingerty, B. E., Broyde, S., and Basu, A. K. (2002) Comparative mutagenesis of the C8-guanine adducts of 1-nitropyrene and 1,6- and 1,8-dinitropyrene in a CpG repeat sequence. A slipped frameshift intermediate model for dinucleotide deletion. *J. Biol. Chem. 277*, 45068–45074.
(8) Djuric, Z., Potter, D. W., Culp, S. J., Luongo, D. A., and Beland, F. A. (1993) Formation of DNA adducts and oxidative DNA damage in rats treated with 1,6-dinitropyrene. *Cancer Lett. 71*, 51–56.
(9) Ohnishi, S., Murata, M., Fukuhara, K., Miyata, N., and Kawanishi, S. (2001) Oxidative DNA damage by a metabolite of carcinogenic 1-nitropyrene. *Biochem. Biophys. Res. Commun. 280*, 48–52.
(10) Heflich, R. H., Fifer, E. K., Djuric, Z., and Beland, F. A. (1985) DNA adduct formation and mutation induction by nitropyrenes in Salmonella and Chinese hamster ovary cells: Relationships with nitroreduction and acetylation. *Environ. Health Perspect. 62*, 135–143.
(11) Fifer, E. K., Heflich, R. H., Djuric, Z., Howard, P. C., and Beland, F. A. (1986) Synthesis and mutagenicity of 1-nitro-6-nitrosopyrene and 1-nitro-8-nitrosopyrene, potential intermediates in the metabolic activation of 1,6- and 1,8-dinitropyrene. *Carcinogenesis 7*, 65–70.
(12) Chumakov, P. (1990) EMBL Data Library, Accession Number ×54156.
(13) Serrano, M., Hannon, G. J., and Beach, D. (1993) A new regulatory motif in cell-cycle control causing specific inhibition of cyclin D/CDK4. *Nature 366*, 704–707.
(14) Capon, D. J., Chen, E. Y., Levinson, A. D., Seeburg, P. H., and Goeddel, D. V. (1983) Complete nucleotide sequences of the T24 human bladder carcinoma oncogene and its normal homologue. *Nature 302*, 33–37.
(15) Yamashita, N., Murata, M., Inoue, S., Hiraku, Y., Yoshinaga, T., and Kawanishi, S. (1998) Superoxide formation and DNA damage induced by a fragrant furanone in the presence of copper(II). *Mutat. Res. 397*, 191–201.
(16) Oikawa, S., Hirosawa, I., Hirakawa, K., and Kawanishi, S. (2001) Site specificity and mechanism of oxidative DNA damage induced by carcinogenic catechol. *Carcinogenesis 22*, 1239–1245.
(17) Yamamoto, K., and Kawanishi, S. (1989) Hydroxyl free radical is not the main active species in site-specific DNA damage induced by copper (II) ion and hydrogen peroxide. *J. Biol. Chem. 264*, 15435–15440.
(18) Murata, M., Mizutani, M., Oikawa, S., Hiraku, Y., and Kawanishi, S. (2003) Oxidative DNA damage by hyperglycemia-related aldehydes and its marked enhancement by hydrogen peroxide. *FEBS Lett. 554*, 138–142.
(19) Maxam, A. M., and Gilbert, W. (1980) Sequencing end-labeled DNA with base-specific chemical cleavages. *Methods Enzymol. 65*, 499–560.
(20) Ito, K., Inoue, S., Yamamoto, K., and Kawanishi, S. (1993) 8-Hydroxydeoxyguanosine formation at the 5′ site of 5′-GG-3′ sequences in double-stranded DNA by UV radiation with riboflavin. *J. Biol. Chem. 268*, 13221–13227.
(21) Levine, A. J., Momand, J., and Finlay, C. A. (1991) The p53 tumour suppressor gene. *Nature 351*, 453–456.
(22) Malaisse, W. J., Hutton, J. C., Kawazu, S., Herchuelz, A., Valverde, I., and Sener, A. (1979) The stimulus-secretion coupling of glucose-induced insulin release. XXXV. The links between metabolic and cationic events. *Diabetologia 16*, 331–341.
(23) Kukielka, E., and Cederbaum, A. I. (1994) Ferritin stimulation of hydroxyl radical production by rat liver nuclei. *Arch. Biochem. Biophys. 308*, 70–77.
(24) Ohnishi, S., Murata, M., and Kawanishi, S. (2002) Oxidative DNA damage induced by a metabolite of 2-naphthylamine, a smoking-related bladder carcinogen. *Jpn. J. Cancer Res. 93*, 736–743.
(25) Kawanishi, S., Hiraku, Y., Murata, M., and Oikawa, S. (2002) The role of metals in site-specific DNA damage with reference to carcinogenesis. *Free Radical Biol. Med. 32*, 822–832.
(26) Stiborova, M., Frei, E., Sopko, B., Sopkova, K., Markova, V., Lankova, M., Kumstyrova, T., Wiessler, M., and Schmeiser, H. H. (2003) Human cytosolic enzymes involved in the metabolic activation of carcinogenic aristolochic acid: Evidence for reductive activation by human NAD(P)H: quinone oxidoreductase. *Carcinogenesis 24*, 1695–1703.
(27) Ritter, C. L., and Malejka-Giganti, D. (1998) Nitroreduction of nitrated and C-9 oxidized fluorenes in vitro. *Chem. Res. Toxicol. 11*, 1361–1367.
(28) Djuric, Z., Potter, D. W., Heflich, R. H., and Beland, F. A. (1986) Aerobic and anaerobic reduction of nitrated pyrenes in vitro. *Chem.-Biol. Interact. 59*, 309–324.
(29) Djuric, Z. (1992) Comparative reduction of 1-nitro-3-nitrosopyrene and 1-nitro-6-nitrosopyrene: Implications for the tumorigenicity of dinitropyrenes. *Cancer Lett. 65*, 73–78.
(30) Kohara, A., Suzuki, T., Honma, M., Oomori, T., Ohwada, T., and Hayashi, M. (2002) Dinitropyrenes induce gene mutations in multiple organs of the lambda/lacZ transgenic mouse (Muta Mouse). *Mutat. Res. 515*, 73–83.
(31) Shibutani, S., Takeshita, M., and Grollman, A. P. (1991) Insertion of specific bases during DNA synthesis past the oxidation-damaged base 8-oxodG. *Nature 349*, 431–434.
(32) Watanabe, T., Takashima, M., Kasai, T., and Hirayama, T. (1997) Comparison of the mutational specificity induced by environmental genotoxin nitrated polycyclic aromatic hydrocarbons in *Salmonella typhimurium* his genes. *Mutat. Res. 394*, 103–112.

TX0497550

Available online at www.sciencedirect.com

SCIENCE DIRECT

Life Sciences 76 (2005) 1439–1453

Life Sciences

www.elsevier.com/locate/lifescie

Mechanism of apoptosis induced by doxorubicin through the generation of hydrogen peroxide

Hideki Mizutani[a,b], Saeko Tada-Oikawa[a], Yusuke Hiraku[a], Michio Kojima[b], Shosuke Kawanishi[a,*]

[a]*Department of Environmental and Molecular Medicine, Mie University School of Medicine, Edobashi, Tsu, Mie 514-8507, Japan*

[b]*Department of Pharmacy, Mie University Hospital, Edobashi, Tsu, Mie 514-8507, Japan*

Received 29 February 2004; accepted 18 May 2004

Abstract

The main anticancer action of doxorubicin (DOX) is believed to be due to topoisomerase II inhibition and free radical generation. Our previous study has demonstrated that TAS-103, a topoisomerase inhibitor, induces apoptosis through DNA cleavage and subsequent H_2O_2 generation mediated by NAD(P)H oxidase activation [H. Mizutani et al. J. Biol. Chem. 277 (2002) 30684-30689]. Therefore, to clarify whether DOX functions as an anticancer drug through the same mechanism or not, we investigated the mechanism of apoptosis induced by DOX in the human leukemia cell line HL-60 and the H_2O_2-resistant sub-clone, HP100. DOX-induced DNA ladder formation could be detected in HL-60 cells after a 7 h incubation, whereas it could not be detected under the same condition in HP100 cells, suggesting the involvement of H_2O_2-mediated pathways in apoptosis. Flow cytometry revealed that H_2O_2 formation preceded the increase in $\Delta\Psi m$ and caspase-3 activation. Poly(ADP-ribose) polymerase (PARP) and NAD(P)H oxidase inhibitors prevented DOX-induced DNA ladder formation in HL-60 cells. Moreover, DOX significantly induced formation of 8-oxo-7,8-dihydro-2′ -deoxyguanosine, an indicator of oxidative DNA damage, in HL-60 cells at 1 h, but not in HP100 cells. DOX-induced apoptosis was mainly initiated by oxidative DNA damage in comparison with the ability of other topoisomerase inhibitors (TAS-103, amrubicin and amrubicinol) to cause DNA cleavage and apoptosis. These results suggest that the critical apoptotic trigger of DOX is considered to be oxidative DNA damage by the DOX-induced direct H_2O_2 generation, although DOX-induced apoptosis may involve topoisomerase II inhibition. This oxidative DNA damage causes indirect

* Corresponding author. Tel./fax: +81 59 231 5011.
E-mail address: kawanisi@doc.medic.mie-u.ac.jp (S. Kawanishi).

0024-3205/$ - see front matter
doi:10.1016/j.lfs.2004.05.040

H_2O_2 generation through PARP and NAD(P)H oxidase activation, leading to the $\Delta\Psi m$ increase and subsequent caspase-3 activation in DOX-induced apoptosis.

Keywords: Doxorubicin; Apoptosis; Hydrogen peroxide; Oxidative DNA damage; 8-oxo-7,8-dihydro-2′ -deoxyguanosine

Introduction

Doxorubicin (DOX), an anthracycline antibiotic, is one of the most popular anticancer drugs. DOX is used for the treatment of human cancers including a variety of solid cancers (Chabner et al., 1996). Although the main anticancer action of DOX is believed to involve DNA damage through topoisomerase II inhibition and free radical generation by redox reaction (Chabner et al., 1996; Gewirtz, 1999; Jung and Reszka, 2001; Hurley, 2002), the mechanism of apoptosis induced by DOX has not well been clarified.

A number of anticancer drugs including DOX exert their effects by inducing apoptosis (Sellers and Fisher, 1999; Kaufmann and Earnshaw, 2000). The major apoptotic pathway of anticancer drugs acts through the loss of mitochondrial membrane integrity (Kaufmann and Earnshaw, 2000). A sudden increase in mitochondrial membrane permeability, so-called mitochondrial permeability transition (MPT), is a central coordination event in the apoptotic process (Mignotte and Vayssiere, 1998; Costantini et al., 2000; Gottlieb, 2000; Kroemer and Reed, 2000). MPT causes the release of cytochrome *c* from mitochondria; cytochrome *c* then activates effector caspases to induce DNA ladder formation. Reactive oxygen species (ROS), such as H_2O_2 and O_2^-, cause apoptosis through MPT (Kroemer et al., 1997; Hampton et al., 1998; Chandra et al., 2000); some anticancer drugs induce ROS formation in apoptosis (Gewirtz, 1999; Muller et al., 1998; Ikeda et al., 1999; Tada-Oikawa et al., 1999; Kajiwara et al., 2001; Mizutani et al., 2002; Nakagawa et al., 2002; Tsang et al., 2003), and we have recently reported that TAS-103, a topoisomerase inhibitor and not a redox agent, induces apoptosis through indirect H_2O_2 generation (Mizutani et al., 2002). However, the mechanism of ROS formation by anticancer drugs including DOX remains to be clarified.

To clarify the mechanism of DOX-induced apoptosis, we investigated apoptosis by examining DNA ladder formation, H_2O_2 generation, mitochondrial membrane potential ($\Delta\Psi m$) change and caspase-3 activation in HL-60 cells and HP100 cells, H_2O_2-resistant cells derived from HL-60. The mechanism of apoptosis was also examined by using inhibitors of poly(ADP-ribose) polymerase (PARP) and NAD(P)H oxidase. Moreover, in order to clarify whether H_2O_2 generation by DOX induces DNA damage, we measured the content of 8-oxo-7,8- dihydro-2′ -deoxyguanosine (8-oxodG), a marker of oxidative DNA damage, in HL-60 and HP100 cells treated with DOX using by high-performance liquid chromatography with an electrochemical detector (HPLC-ECD). In addition, we compared the ability of DOX to cause DNA damage and DNA ladder formation with that of topoisomerase inhibitors [TAS-103, amrubicin (AMR) and amrubicinol (AMR-OH), an active metabolite of AMR]. AMR is a new, completely synthetic 9-aminoanthracycline derivative which induces anticancer effects by stabilizing topoisomerase II-DNA complex (Hanada et al., 1998).

Material and methods

Materials

DOX was purchased from Wako Pure Chemical Industries (Osaka, Japan). TAS-103 was provided by Taiho Pharmaceutical Co., Ltd (Tokyo, Japan). AMR and AMR-OH were provided by Sumitomo Pharmaceutical Co., Ltd (Osaka, Japan). Proteinase K was obtained from Merck (Darmstadt, Germany). 2′,7′-Dichlorofluorescin diacetate (DCFH-DA) and 3,3′-dihexyloxacarbocyanine iodide [$DiOC_6(3)$] were purchased from Molecular Probes (Eugene, OR). z-Asp-Glu-Val-Asp-7-amino-4-trifluoromethyl coumarin (DEVD-AFC) and diphenyleneiodonium chloride (DPI) were provided by Biomol (Plymouth Meeting, PA). 6(*5H*)-Phenanthridinone (PHEN) was obtained from Wako Pure Chemical Industries Ltd. (Osaka, Japan). Apocynin (APO) was purchased from Nacalai Tesque, Inc. (Kyoto, Japan). ^{32}P-labeled DNA fragment was also obtained from the human c-Ha-*ra*s-1 protooncogene (Mizutani et al., 2003).

Cell culture and treatment with DOX

HP100 cells have been derived from human leukemia HL-60 cells by repeated exposure to H_2O_2, followed by outgrowth of viable cells, and were approximately 340-fold more resistant to H_2O_2 than HL-60 cells (Kasugai and Yamada, 1989). Catalase activity of HP100 cells is 18 times higher than that of HL-60 cells (Kasugai and Yamada, 1992). HL-60 and HP100 cells were grown in RPMI 1640 supplemented with 6% fetal calf serum at 37 °C under 5% CO_2 in a humidified atmosphere. The cells (1×10^6 cells/ml) were then treated with the indicated concentrations of DOX. Cells were preincubated with either PARP inhibitors or NAD(P)H oxidase inhibitors for 0.5 h where indicated.

Detection of apoptosis induced by DOX

For analysis of DNA ladder formation by treatment with DOX, cells were washed twice with PBS. Cells (2×10^6 cells), resuspended in 1 ml cytoplasm extraction buffer [10 mM Tris (pH 7.5), 150 mM NaCl, 5 mM $MgCl_2$ and 0.5% Triton X-100], were centrifuged at $1000 \times g$ for 5 min at 4 °C. The cellular pellet was resuspended in lysis buffer [10 mM Tris (pH 7.5), 400 mM NaCl and 1 mM EDTA] and centrifuged at $12{,}000 \times g$ for 10 min at 4 °C. The supernatant was then treated overnight with 0.2 mg/ml RNase at room temperature, followed by treatment with proteinase K as described previously (Hiraku and Kawanishi, 1996). DNA ladder formation was analyzed by conventional electrophoresis.

Flow cytometric detection of peroxide and $\Delta\Psi m$ in cells treated with DOX

To evaluate cellular peroxide levels, DOX-treated cells were incubated with 5 μM DCFH-DA for 30 min at 37 °C (Xiang et al., 1996). To assess changes in $\Delta\Psi m$, DOX-treated cells were incubated with 40 nM $DiOC_6(3)$ for 15 min at 37 °C (Decaudin et al., 1997). Cells were then washed twice with PBS. Following resuspension in PBS, the cells were analyzed on a flow cytometer (FACScan; Becton Dickinson, San Jose, CA). Dead cells and debris were excluded from

the analysis. The data were analyzed using the data analysis program, Cell Quest (Becton Dickinson).

Measurement of caspase-3 activity

To analyze caspase-3 activity, DOX-treated cells (1×10^6 cells) were washed twice with PBS and resuspended in a 100 μl solution containing 0.1 M HEPES (pH 7.4), 2 mM dithiothreitol, 0.1% CHAPS, and 1% sucrose. Cell suspensions were first frozen in liquid nitrogen and then thawed at 37 °C. This freeze-thaw procedure was repeated three times. Cell lysates were then centrifuged at 18,500 × *g* for 15 min, to obtain the apoptotic extracts. The reaction was initiated by the addition of 20 μM DEVD-AFC, a caspase-3 substrate, to 50 μl apoptotic extract at 37 °C. Product formation was measured using a Shimadzu RF-5300PC spectrofluorometer (Kyoto, Japan) with excitation at 400 nm and emission at 505 nm (Hishita et al., 2001).

Measurement of 8-oxodG in cultured cells

Cells (1×10^6 cells/ml) were incubated with DOX at 37 °C and immediately washed three times with PBS. Under anaerobic conditions, DNA was extracted using lysis buffer, RNase A and proteinase K. After ethanol precipitation, DNA was digested to component nucleosides with nuclease P_1 and bacterial alkaline phosphatase and the resulting mixture was analyzed by HPLC-ECD, as described previously (Ito et al., 1993).

Analysis of DNA damage by DOX, AMR, AMR-OH or TAS-103 in the presence of Cu(II)

The reaction mixture in a microtube (1.5 ml Eppendorf) contained 10 μM drugs, 20 μM $CuCl_2$, ^{32}P-labeled DNA fragment and calf thymus DNA (2 μM/base) in 200 μl of 10 mM sodium phosphate buffer (pH 7.8) containing 5 μM DTPA, a chelating agent, to remove trace amounts of contaminated metals. After incubation at 37 °C for 60 min, the DNA fragments were treated with 1 M piperidine at 90 °C for 20 min, and then electrophoresed on an 8% polyacrylamide/8 M urea gel. The autoradiogram was obtained by exposed X-ray film to the gel (Mizutani et al., 2003).

Results

DNA ladder formation in HL-60 and HP100 cells treated with DOX

We have analyzed DNA ladder formation, which is characteristic for apoptosis, in the cells treated with DOX using conventional electrophoresis. The DNA ladder formation could be detected at 1-5 μM in HL-60 cells after an 8 h incubation, whereas it could be detected apparently at 2–5 μM in HP-100 cells. (Fig. 1A). The time-course of the DNA ladder formation by 1 μM DOX was shown in Fig. 1B. It was detectable at 7 h in HL-60 cells, whereas it was observed slightly at 8 h in HP100 cells. The cell viability at 8 h estimated by trypan blue exclusion was 80% and 90 % at 1 μM in HL-60 and HP100 cells, respectively.

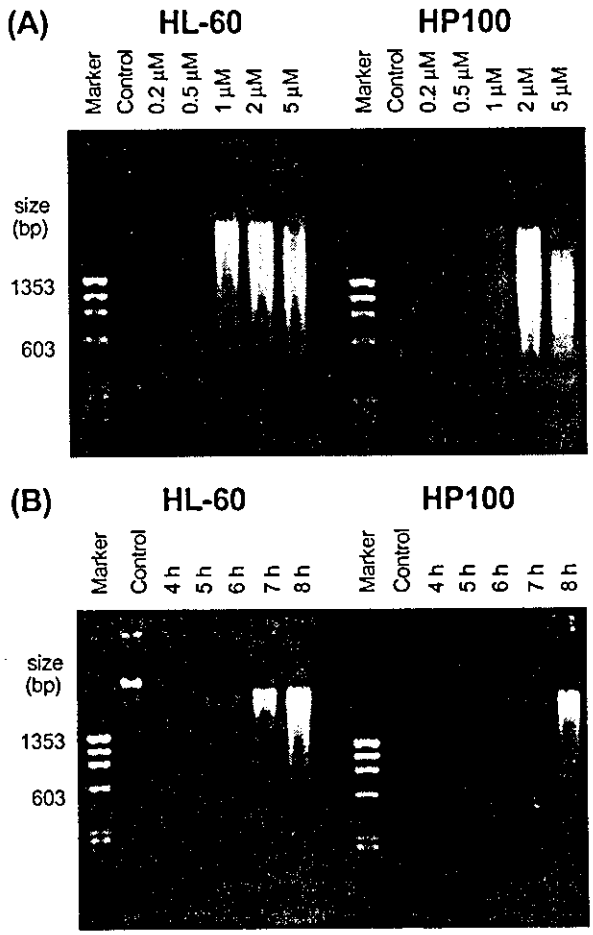

Fig. 1. Detection of DNA ladder formation in HL-60 and HP100 cells treated with DOX. (A) HL-60 and HP100 cells (1×10^6 cells/ml) were treated with DOX at 37 °C for 8 h. (B) HL-60 and HP100 cells (1×10^6 cells/ml) were treated with 1 μM DOX at 37 °C for the indicated times. The cells were lysed, and DNA was extracted and analyzed by conventional electrophoresis. Marker lane: size marker DNA (ΦX174/*Hae* III digest).

Generation of peroxide and change of ΔΨm in HL-60 and HP100 cells treated with DOX

In Fig. 1A, the DNA ladder formation could be detected apparently at 1 μM in HL-60 cells. Therefore, we performed the time-course experiments of DOX-induced apoptotic events at 1 μM to reveal difference between HL-60 and HP100 cells. As shown in Fig. 2, peroxide generation in HL-60 cells was apparently observed at 1 h after the treatment with DOX, while its generation in HP100 cells was not observed. Fig. 3 shows change of ΔΨm in HL-60 and HP100 cells treated with DOX to examine whether DOX induces MPT. ΔΨm in HL-60 was slightly increased at 4 h, and apparently at 6 h. No increase in ΔΨm was observed in HP100 at 4 h, and ΔΨm increased slightly at 6 and 8 h in comparison with HL-60 cells.

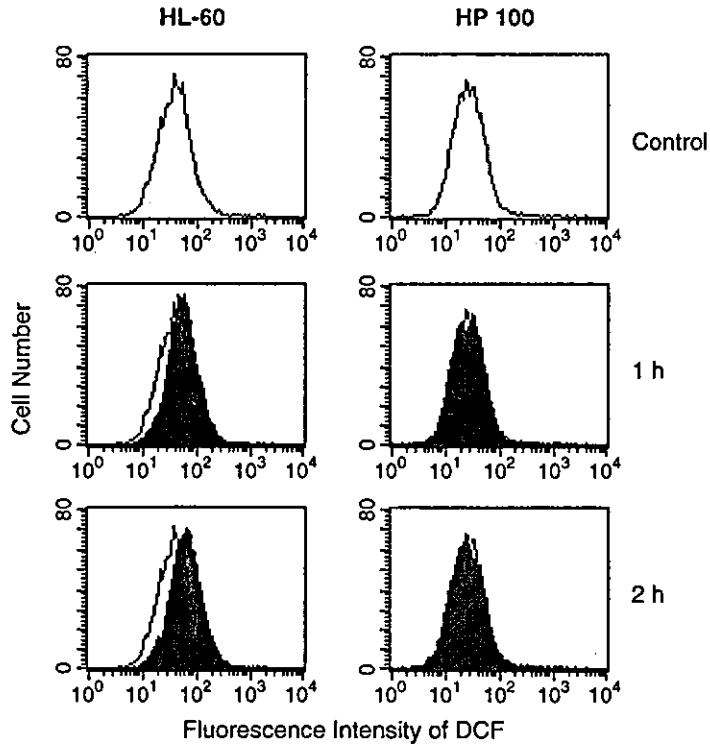

Fig. 2. Generation of H_2O_2 in HL-60 and HP100 cells treated with DOX. HL-60 and HP100 cells (1×10^6 cells/ml) were treated with 1 μM DOX at 37 °C for the indicated times. After the treatment, the cells were incubated with 5 μM DCFH-DA for 30 min at 37 °C. The cells were analyzed with a flow cytometer (FACScan). Open peaks, control; shaded peaks, DOX-treated cells.

Activation of caspase-3 by DOX in HL-60 and HP100 cells treated with DOX

Activation of caspase-3 in DOX-treated cells was measured using a fluorometric assay with its substrate DEVD-AFC. The caspase-3 activity was increased after treatment with DOX for 7 h in HL-60 and HP100 cells. Caspase-3 activity in HL-60 was significantly higher than that seen in HP100 at 8 h (Fig. 4).

Inhibitory effects of PARP and NAD(P)H oxidase inhibitors on apoptotic process in HL-60 cells treated with DOX

PARP is a DNA repair enzyme activated by DNA cleavage (Bertrand et al., 1993; Scovassi and Poirier, 1999; Martin et al., 2000). NAD(P)H oxidase mediates peroxide generation (Jones et al., 2000). Thus, we investigated the effects of PARP and NAD(P)H oxidase inhibitors on DNA ladder formation in HL-60 cells treated with DOX. PARP inhibitors (ANI and PHEN) and NAD(P)H oxidase inhibitors (DPI and APO) prevented DOX-induced DNA ladder formation (Fig. 5), indicating that this apoptosis occurs through the activation of PARP and NAD(P)H oxidase. In addition, we analyzed the effects of ANI and DPI on peroxide generation and the change in $\Delta\Psi m$ following the treatment of HL-60 cells with DOX.

ANI did not inhibit peroxide production at 2 h and the change in $\Delta\Psi m$ at 4 h. DPI, a flavoenzyme inhibitor, which inhibits not only NAD(P)H oxidase but also NADPH-cytochrome P450 redutase (Tew, 1993; Ramji et al., 2003), suppressed peroxide production. DPI increased the change in $\Delta\Psi m$ (Fig. 6).

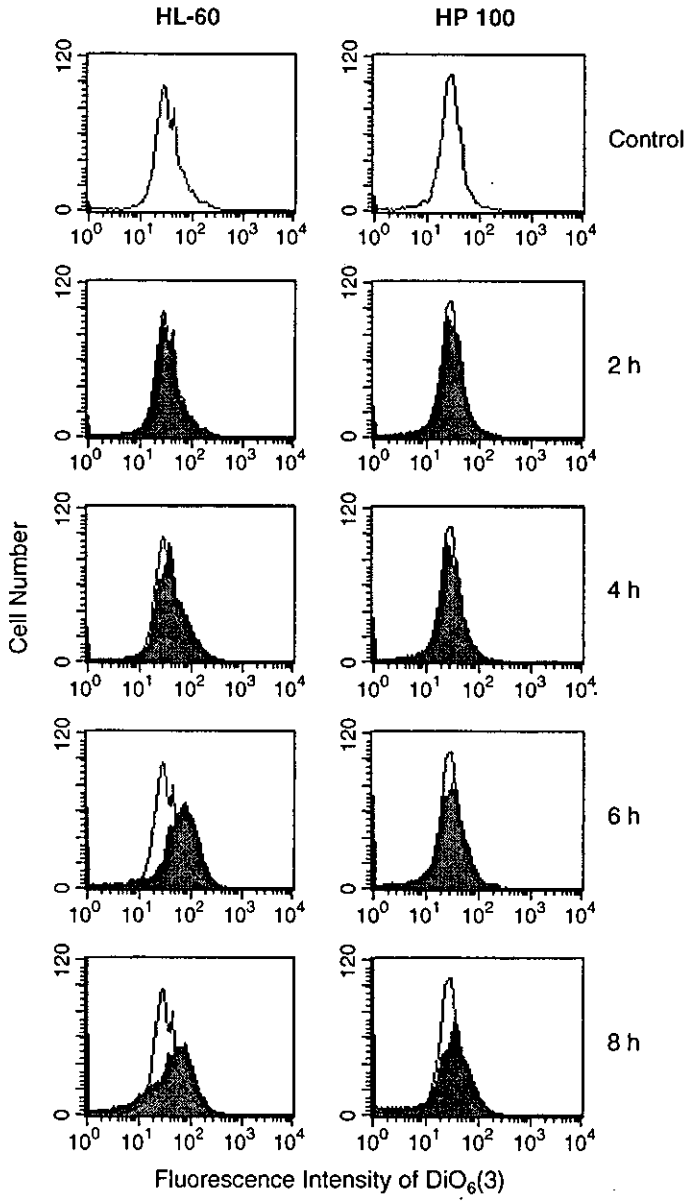

Fig. 3. Change of mitochondorial membrane potential in HL-60 and HP100 cells treated with DOX. HL-60 and HP100 cells (1×10^6 cells/ml) were treated with DOX at 37 °C for the indicated times. After the treatment, the cells were incubated with 40 nM $DiOC_6(3)$ for 15 min at 37 °C. The cells were analyzed with a flow cytometer (FACScan). Open peaks, control; shaded peaks, DOX-treated cells.

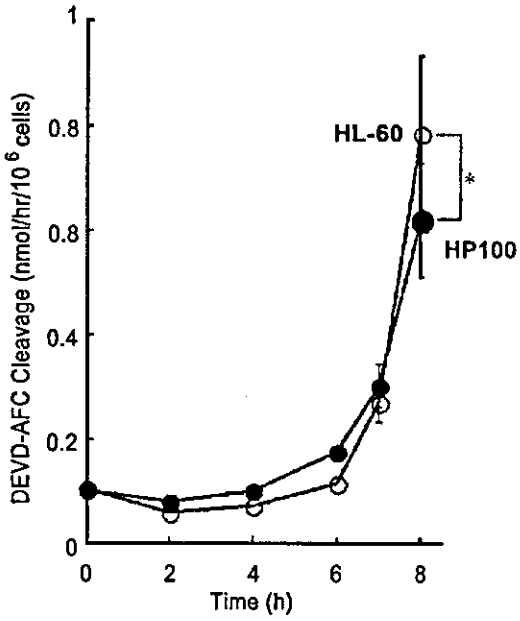

Fig. 4. Activation of caspase-3 in HL-60 and HP100 cells treated with DOX. Caspase-3 activity was measured by cleavage of DEVD-AFC, using extracts of HL-60 (○) and HP100 (●) cells undergoing DOX-induced apoptosis. The cells (1×10^6 cells/ml) were treated with 1 μM DOX at 37 °C for the indicated times. Results represent means ± SD of five independent experiments. Asterisks indicate significant differences between HL-60 cells and HP100 cells by *t*-test (* $P < 0.05$).

Formation of 8-oxodG in HL-60 and HP100 cells treated with DOX

We investigated 8-oxodG formation in HL-60 and HP100 cells. DOX significantly induced 8-oxodG formation in HL-60 cells, whereas no significant 8-oxodG formation compared with the control was

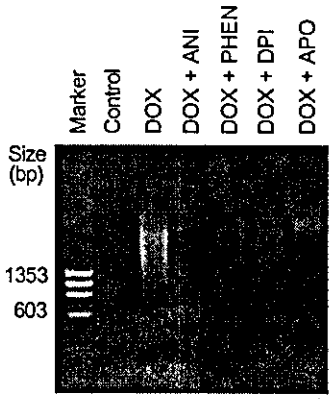

Fig. 5. Inhibitory effects of PARP inhibitors and NAD(P)H oxidase inhibitors on DNA ladder formation in HL-60 cells treated with DOX. HL-60 cells (1×10^6 cells/ml) were treated with 1 μM DOX at 37 °C for 8 h. Cells were preincubated for 0.5 h with 20 μM ANI, 100 μM PHEN, 2 μM DPI, or 1 mM APO, where indicated. Following lysis, DNA was extracted and analyzed by conventional electrophoresis. Marker lane: size marker DNA (ΦX 174/*Hae* III digest).

observed in HP100 cells under the same conditions, suggesting that H_2O_2-mediated oxidative DNA damage was induced (Fig. 7).

Damage to ^{32}P-labeled DNA fragments by DOX, AMR, AMR-OH and TAS-103 in the presence of Cu(II)

Recently, we have reported DOX-induced DNA damage in the presence of Cu(II) (Mizutani et al., 2003). Thus, we compared DOX-induced DNA damage with that by two other topoisomerase inhibitors

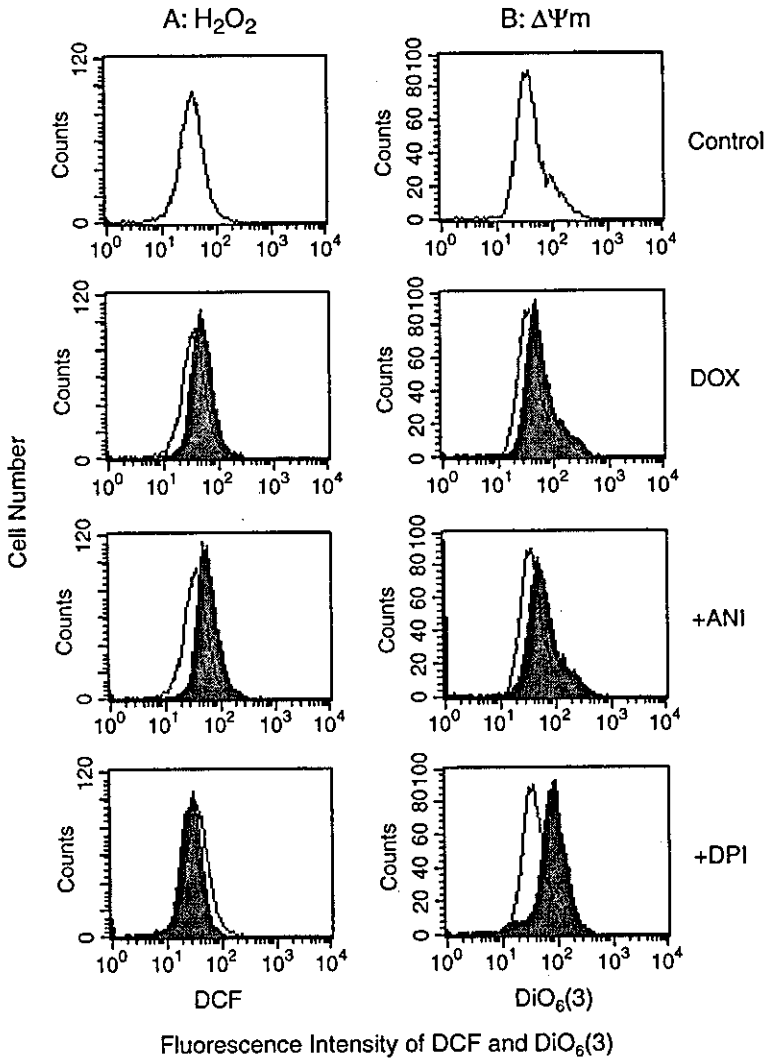

Fig. 6. Effects of ANI and DPI on peroxide generation and changes in ΔΨm following the treatment of HL-60 cells with DOX. HL-60 cells (1×10^6 cells/ml) were treated with 1 μM DOX at 37 °C for 2 h (A) or 4 h (B). Cells were preincubated for 0.5 h with 20 μM ANI or 2 μM DPI, where indicated. After the treatment, the cells were incubated with 5 μM DCFH-DA for 30 min (A) or 40 nM $DiOC_6(3)$ for 15 min (B) at 37 °C. The cells were analyzed with a flow cytometer (FACScan). Open peaks, control; shaded peaks, DOX-treated cells.

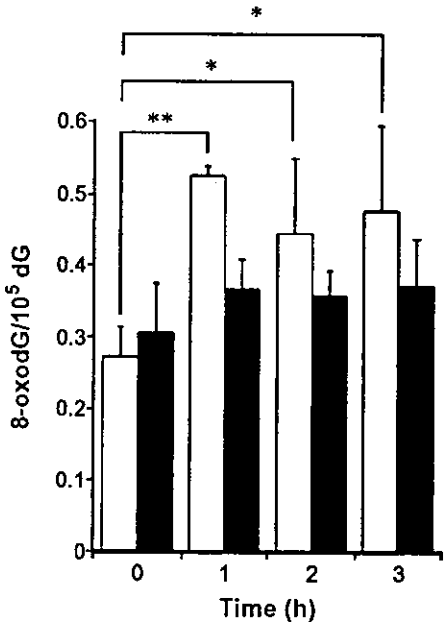

Fig. 7. Formation of 8-oxodG in HL-60 and HP100 cells treated with DOX. HL-60 (□) and HP100 (■) cells (1×10^6 cells/ml) were treated with 1 μM DOX at 37 °C for the indicated times. After the treatment, DNA was extracted and subjected to enzyme digestion and analyzed by an HPLC-ECD. Values represent means ± SD of three independent experiments. Asterisks indicate significant differences compared with control by *t*-test (* $P< 0.05$, ** $P< 0.01$).

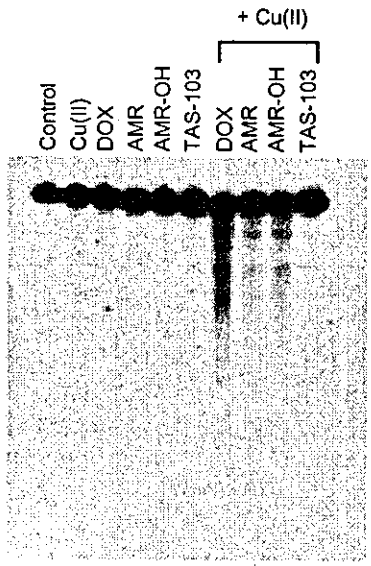

Fig. 8. Autoradiogram of ^{32}P-labeled DNA fragment incubated with DOX, AMR, AMR-OH and TAS-103 in the presence of Cu(II). The reaction mixture contained the ^{32}P-5′ -end-labeled 261-bp fragment, 2 μM/base of calf thymus DNA, 20 μM $CuCl_2$ and 10 μM reagents in 200 μl of 10 mM phosphate buffer (pH 7.8) containing 2.5 μM DTPA. The mixture was incubated at 37 °C for 60 min. The DNA fragments were treated with piperidine and analyzed by the method described under Materials and Methods.